Gene expression associated with intersterility in *Heterobasidion.*

Van der Nest, M.A[1]*., Olson, Å.[1], Karlsson, M.[1], Lind, M[1]., Dalman., K.[1], Brandström-Durling, M.[1], Elfstrand, M.[1], Wingfield, B.D.[2] and Stenlid, J[1].

[1]Department of Forest Mycology and Plant Pathology, Swedish University of Agricultural Sciences, Uppsala, SE-750 07, Sweden; [2]Department of Genetics, Forestry and Agricultural Biotechnology Institute (FABI), University of Pretoria, Pretoria, 0002, South Africa.

*Corresponding author (Current address):
E-mail: magriet.vandernest@fabi.up.ac.za
Tel: +27-12-420-3906
Fax: +27-12-420-3960
Department of Genetics
Forestry and Agricultural Biotechnology Institute (FABI)
74 Lunnon Road, Hillcrest
Pretoria, 0002
South Africa

Abstract

Intersterility (IS) is thought to prevent mating compatibility between homokaryons that belong to different species. Although IS in *Heterobasidion* is regulated by the genes located at the IS loci, it is not yet known how the IS genes influence sexual compatibility and heterokaryon formation. To increase our understanding of the molecular events underlying IS, we studied mRNA abundance changes during IS compatible and incompatible interactions over time. The clustering of the transcripts into expression profiles, followed by the application of Gene Ontology (GO) enrichment pathway analysis of each of the clusters, allowed inference of biological processes participating in IS. These analyses identified events involved in mating and sexual development (i.e., linked with IS compatibility), which included processes associated with cell-cell adhesion and recognition, cell cycle control and signal transduction. We also identified events potentially involved in overriding mating between individuals belonging to different species (i.e., linked with IS incompatibility), which included reactive oxygen species (ROS) production, responses to stress (especially to oxidative stress), signal transduction and metabolic biosynthesis. Our findings thus enabled detection and characterization of gene expression changes associated with IS in *Heterobasidion*, as well as identification of important processes and pathways associated with this phenomenon. Overall,

the results of this study increase current knowledge regarding the molecular mechanisms underpinning IS in *Heterobasidion* and allowed for the establishment of a vital baseline for further studies.

Keywords:
Heterobasidion occidentale, Heterobasidion irregulare, Intersterility, Mating, RNA-seq.

1. INTRODUCTION

Heterobasidion annosum (Fr.) Bref. *sensu lato* (s.l.), the causal agent of annosus root rot, is associated with significant economic losses to forest owners in the Northern Hemisphere (Bendz-Hellgren and Stenlid, 1997). This important fungal complex consists of several species with different host preferences. In Europe, *H annosum sensu stricto* (s.s.) occurs mainly on pine (*Pinus* species), *H. parviporum* on spruce (*Picea* species), and *H. abietinum* on fir (*Abies* species), while in North America, *H. occidentale* on *Abies*, *Pseudotsuga* and *Tsuga* and *H. irregulare* on *Pinus* and *Juniperus* species (Korhonen et al., 1997, 1998; Otrosina and Garbelotto, 2010).

Heterobasidion species are mushroom-forming fungi with a typical Basidiomycetes life cycle that consist of a short homokaryotic phase (i.e., where one type of haploid nuclei inhabit the mycelium) followed by a heterokaryotic phase (i.e., where two or more genetically different haploid nuclei inhabit the mycelium) (Chase and Ullrich, 1990a). Under appropriate environmental conditions the heterokaryotic mycelium forms basidiocarps (fruiting bodies), which produce airborne sexual spores (basidiospores) (Möykkynen et al., 1997). Germinated basidiospores give rise to homokaryotic hyphae that can fuse to again establish the heterokaryotic phase, but only when the interacting homokaryons are sexually compatible (Heitman et al., 2007).

Sexual reproduction in *Heterobasidion* is characterized by a heterothallic bipolar mating system, which is controlled by the *mat-A* locus that encodes two classes of homeodomain transcription factors (Olson et al., 2012; van Diepen et al., 2013). Apart from controlling mate recognition, these proteins also control nuclear division and the formation of clamp connections (Heitman et al., 2007). Although not involved in mate recognition, the *Heterobasidion* genome

also harbours the *mat-B* locus (Olson et al., 2012), which encode G-protein coupled pheromone receptors and pheromones that are most likely involved in the pheromone-signalling cascade controlling nuclear migration and clamp connection fusion (e.g., Olesnicky et al., 1999). In *Heterobasidion*, the mating type genes located at the *mat-A* and *mat-B* loci are therefore thought to be necessary for mating and heterokaryon formation, although mating specificity is determined by the *mat-A* locus.

Intersterility (IS) is a type of heterospecific non-self recognition that prevents mating compatibility between homokaryons belonging to different species (e.g., Korhonen, 1978; Chase and Ullrich, 1990a; Garbelotto et al., 2004). IS in *Heterobasidion* is controlled by a bi-allelic (+ or – alleles) system consisting of five genes, referred to as S, P, V_1, V_2, and V_3 (Chase and Ullrich, 1990a, 1990b; Olson and Stenlid, 2001; Lind et al., 2005). Two homokaryons are IS compatible if they have a common + allele at least at one of the IS loci. For example, all *H. occidentale* homokaryons share a + allele at the S locus, while *H. irregulare* homokaryons share a + allele at the P locus (Chase and Ullrich, 1990a; Garbelotto et al., 2007). The sterility barrier is not always complete, with *H. occidentale* and *H. irregulare* homokaryons sometimes being able to mate. This is possibly controlled by one or more of the other IS genes (i.e., V_1, V_2, and V_3) (Stenlid and Karlsson, 1991; Garbelotto et al., 2004, 2007; Lind et al., 2005). It is not known, however, how the IS genes influence mating and heterokaryon formation in *Heterobasidion*.

Despite the apparent overlap in the processes controlled by the *mat* and the IS loci, sexual compatibility and IS play markedly different evolutionary roles. The products of the *mat* loci influence the degree of inbreeding *vs.* outbreeding within a population, while the IS loci act to restrict gene flow between species (Chase and Ullrich, 1990a, 1990b; Garbelotto et al., 2004). It is believed that IS in *Heterobasidion* functions as a reproductive barrier between closely related species and is driven by extrinsic post-zygotic isolation (i.e., where hybrids have reduced mating success) (Garbelotto et al., 2007; Olson, 2006). Restricted gene flow between closely related species, together with natural selection, may have resulted in the isolation and host specialization of *Heterobasidion* species (Korhonen, 1978; Chase and Ullrich, 1990a; Oliva et al., 2011). In turn, host preference may limit gene flow between closely related *Heterobasidion* species, as it could act as a barrier for inter-specific crossings (Korhonen, 1978; Chase and Ullrich, 1990a; Oliva et al., 2011). This association between IS and host specialization in *Heterobasidion* could suggest that pathogenicity in these fungi is mediated by

genes physically or genetically linked to the IS loci or is directly mediated by the S and P IS genes themselves (Chase and Ullrich, 1990a; Lind et al., 2005; Olson, 2006).

Although the molecular biology of sexual compatibility and mating is relatively well understood in the Basidiomycetes, little is known about the processes and pathways underlying IS. The availability of a high-quality genomic reference for *H. irregulare* (Olson et al., 2012), along with advances in high-throughput sequencing technologies and bioinformatics (e.g., Kircher et al., 2011) present ample opportunities for increasing the current IS knowledge-base. Our overall goal was to study the molecular responses underlying IS by comparing patterns of gene expression in compatible and incompatible IS interactions over time. The major objectives were to identify and characterize functional changes associated with the expression of genes during IS, and to identify important processes and pathways underpinning IS to infer how they are linked with the biology of these fungi.

2. MATERIALS AND METHODS

2.1. Fungal strains, IS interactions and experimental design

In this study we utilized hybrid progeny (strains AO8-5, AO8-25, AO8-48 and AO8-73) of the parental strains TC 122-12 (*H. occidentale,* IS genotype $S^{+}P^{-}V_1^{-}V_2^{-}V_3^{+}$) and TC 32-1 (*H. irregulare*, IS genotype $S^{-}P^{+}V_1^{n}V_2^{+}V_3^{+}$) (Chase, 1986; Olson and Stenlid, 2001; Lind et al., 2005). We also included the mating tester strain Så 16-4 (IS genotype $S^{-}P^{+}V_1^{-}V_2^{-}V_3^{-}$) used to genotype the parent and hybrid progeny (Lind et al., 2005). Working cultures of the isolates were maintained on Hagem agar (HA, Stenlid, 1985) and stored at 4 ˚C.

The tester strain Så 16-4 was paired separately with the hybrid progeny AO8-5 and AO8-25 that carry the $^{-}$ allele for the P locus (i.e., they are intersterile and IS incompatible), as well as with hybrid progeny AO8-48 and AO8-73 that carry the $^{+}$ allele for the P locus (i.e., they are interfertile and IS compatible) (Fig. 1). This was done by placing a mycelial plug (5 mm in diameter) of each isolate 3 cm apart in the middle of a 9 cm Petri dish containing HA followed by incubation in the dark at 25 ˚C. To study the molecular response during IS over time, mycelia were harvested from the interaction zone at 12, 24 and 96 h after the establishment of hyphal contact and frozen in liquid nitrogen.

Table 1. Summary of sequence reads.

Interaction	Time (hours post hyphal contact)	Number of raw reads	Number of reads after filtering[a]
IS Incompatible			
Så 16.4 x A08-5	12	58 963 070	50 515 168
Så 16.4 x A08-5	48	47 605 530	43 443 162
Så 16.4 x A08-5	96	80 936 590	73 582 244
Så 16.4 x A08-25	12	30 692 420	27 789 900
Så 16.4 x A08-25	48	69 874 338	60 273 013
Så 16.4 x A08-25	96	51 420 064	44 109 622
IS Compatible			
Så 16.4 x A08-48	12	52 881 526	48 005 479
Så 16.4 x A08-48	48	38 037 720	34 432 438
Så 16.4 x A08-48	96	79 967 776	72 487 138
Så 16.4 x A08-73	12	33 762 284	30 693 718
Så 16.4 x A08-73	48	104 080 250	89 260 343
Så 16.4 x A08-73	96	41 290 500	36 993 311

[a] The software package CLC Genomics Workbench 6.0.1 (CLCbio, Aarhus, Denmark) was used to filter Illumina reads based on limit quality scores using a phred scale of 20, to remove adapter sequences from reads, as well as to discard poor-quality terminal bases. The average read length of the samples after trimming ranged between 77.6 and 78.1 nucleotides.

Figure 1. Schematic illustration of the experimental design used to study intersterility (IS) in Heterobasidion. For the incompatible IS interactions the tester strain Så 16-4 was paired separately with A08-5 and A08-25, that are IS incompatible and carry the - allele for the P locus. For the compatible IS interactions, Så 16-4 was paired separately with A08-48 and A08-73 that are IS compatible and carry the + allele for the P locus. Mycelium was harvested from the interacting zone of the IS compatible and incompatible interactions for RNA-seq analysis (indicated with the grey block).

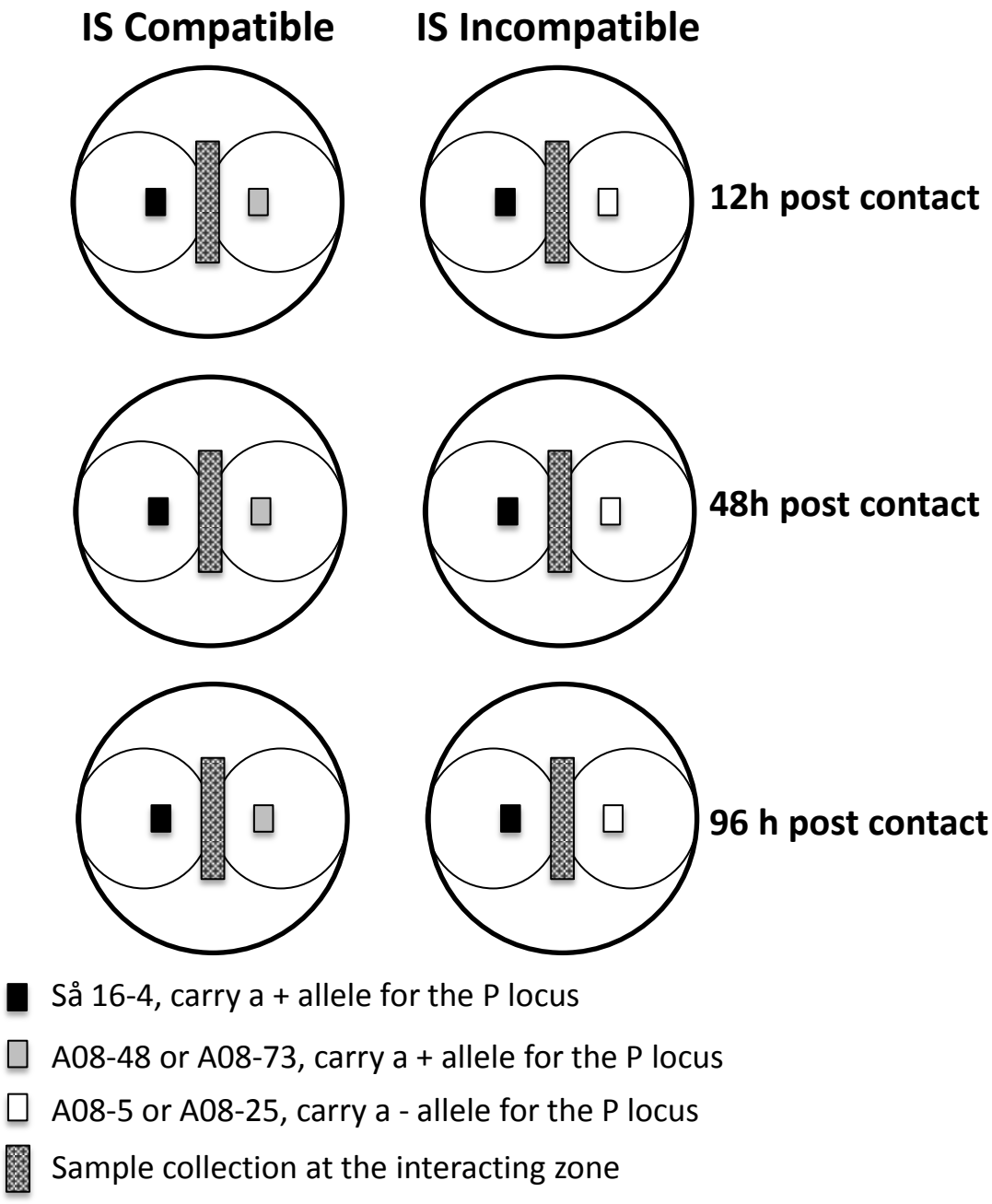

Each sample used in the expression study represented the pooled mycelium harvested from 3 biological replicates, since it has been shown that pooling of samples allows for biological averaging (Kendziorski et al., 2005). Also, in order to test the statistical significance of differential expression between experiments, each interaction was replicated in two individuals (i.e., the two strains with the same IS genotype). The samples that we compared in this study thus included 6 groups, each consisting of two replicates (Fig. 1). These were the IS compatible (interfertile) interactions Så 16-4 x AO8-48 and Så 16-4 x AO8-73 at each of the three time points (12h, 48h and 96h), and the IS incompatible (intersterile) interactions Så 16-4 x AO8-5 and Så 16-4 x AO8-25 at each of the three time points (Table 1).

2.2. RNA extraction, high-throughput sequencing and RNA-seq analysis

High quality total RNA (RNA Integrity Number, RIN >7; Schroeder et al., 2006) was extracted using the RNeasy® Mini Kit (Qiagen, Valencia, CA, USA) and genomic DNA was removed with DNAse (Thermo Scientific, Germany) treatment, following the manufacturer's instructions. Quantity and quality of total RNA were assessed by measurement of absorbance using a NanoDropND/1000 UV spectrophotometer (Thermo Fisher Scientific, Germany) and capillary electrophoresis in an RNA Pico 6000 chip using an Agilent Bioanalyzer 2100 System (Agilent Technologies, USA). mRNA isolation, mRNA purification and mRNA fragmentation, as well as cDNA synthesis was performed at the SNP&SEQ Technology Platform of Uppsala University Hospital. High-throughput sequencing was also performed at the SNP&SEQ Technology Platform of Uppsala University Hospital using the Illumina Genome Analyzer (Illumina, San Diego, CA, USA) according to standard protocols. Image analysis and base calling were performed using the analysis pipe-line supplied with the Genome Analyzer instrument. The samples were sequenced for 'paired-end' reads across one Illumina lane.

The software package CLC Genomics Workbench 6.0.1 (CLC bio, Aarhus, Denmark) was used to filter the Illumina reads based on a phred-scale quality score cut-off of 20. This software was also used to remove adapter sequences from reads and to discard poor-quality reads and/or terminal nucleotides. We then used the CLC Genomics Workbench to align the filtered and/or trimmed sequence reads to the annotated *H. irregulare* reference genome (Olson et al., 2012; DOE Joint Genome Institute, JGI, http://genome.jgi.doe.gov/). To ensure optimal alignment and to allow for sequence divergence between *H. irregulare* and *H. occidentale*, we used a filtering threshold of 0.5 for the length fraction and a similarity parameter value of 0.8. In other words, at least 50 % of an individual read needed to match the reference sequence at a

similarity of >80 % for the read to be included in the final mapping.

Comparisons of expression levels between samples were done according to Mortazavi et al. (2008). This entailed normalization of the data in each sample by dividing the number of reads mapping to each gene by the length of the gene and by the total number of reads sequenced across the transcriptome (Reads Per Kilobase per Million mapped reads, or RPKM). We also employed a quantile normalization algorithm on the RPKM values to account for technical variability in RNA-seq data (Hansen et al., 2012). Baggerley's Z test on expression proportions was utilized to test for RPKM differences between samples (Baggerley et al., 2003). This test compares the proportions of counts in a group of samples (i.e., the IS compatible or incompatible interactions at one of the three time points) against those of another group of samples, where the samples are given different weights depending on their sizes (total counts). The weights are obtained by assuming a Beta distribution on the proportions in a group, and estimating these, along with the proportion of a binomial distribution, by the method of moments. The result is a weighted t-type test statistic. To minimize gene expression measurement errors, statistical significance was assessed using *P*-values adjusted for multiple test correction using the Benjamini-Hochberg false discovery rate (FDR) method (Benjamini and Hochberg, 1995). In this study, we used a conservative threshold for identifying differentially expressed (DE) genes, thereby ignoring genes that have smaller effects. We considered genes to be DE only if they displayed a two-fold change in expression at a FDR cut-off value of 0.05 (i.e., 2.0 fold change at FDR $q \leq 0.05$).

2.3. Gene clustering and Functional annotation

Gene Cluster version 3.0 (de Hoon et al., 2004) was employed to identify trends within the datasets based on similarity in expression patterns, using the DE genes as input (i.e., the DE transcripts in at least one of the 6 samples studied). The data was median-centred and submitted to hierachical clustering using pairwise average linkage clustering analysis. We visualized the results with TreeView version 1.6.6 (Page, 1996).

BLAST2GO (http://www.blast2go.org) was used to annotate the DE genes in each cluster, as well as assessing Gene Ontology (GO) term enrichment. The Fisher exact tests in the BLAST2GO program were employed using default settings to identify significantly ($P \leq 0.05$) enriched terms, where the significance value for each GO term reflects the enrichment in frequency of that GO term in the input entity list relative to all of the GO terms of the complete

H. irregulare transcriptome (Conesa et al., 2005). The process(es) associated with these terms were also summarized using the REVIGO web server that condenses the GO descriptions by removing redundant terms (http://revigo.irb.hr/). In this study we only included the significantly enriched GO terms (with a *P*-value of ≤ 0.05) and utilized REVIGO's "small allowed similarity" setting, in order to obtain a more compact output.

We investigated the cytochrome P450 monooxygenase (CYP) genes in *H. irregulare* in more depth because of the presence of a putative gene cluster associated with secondary metabolite biosynthesis, as well as the fact that a large number of the DE genes encoded CYPs (Supplementary Table 11). For this purpose, a UPGMA (Unweighted Pair Group Method with Arithmetic mean) tree was constructed using the *H. irregulare* CYP sequences obtained from the JGI database (http://genome.jgi.doe.gov/), as well as previously characterized CYP sequences (http://drnelson.uthsc.edu/CytochromeP450.html). The amino acid sequences were aligned using MAFFT version 7 and the tree constructed using MEGA version 6 (http://www.megasoftware.net).

3. RESULTS

3.1. RNA-seq analysis

Illumina HiSeq sequencing of the *Heterobasidion* libraries produced 30 692 420 to 104 080 250 reads with an average length of 100 nucleotides (Table 1). After quality trimming and filtering, the number of reads ranged between 27 789 900 and 89 260 343, with an average length of 78 nucleotides (Table 1). Our mapping approach allowed efficient alignment of the reads generated for the respective samples to the *H. irregulare* reference genome, with 91 % of the reads mapping to the reference. The unmapped reads may be the result of sequences being specific to *H. occidentale*, sequencing errors, the presence of polyA sequences or reads that come from repetitive sequence (Marioni et al 2008; Huang and Khatib, 2010). A large proportion of the reads mapped to non-coding regions (i.e., untranslated regions of genes; results not shown) or potentially to incorrectly annotated regions (Marioni et al 2008). This is because only *ca*. 69 % of all the reads mapped uniquely to annotated exons of the *H. irregulare* reference genome, which is consistent with what has been reported for other eukaryotes; e.g., yeast with 56 % mapped (Nagalakshmi et al., 2008) and humans with 60-65 % mapped (Degner et al., 2009).

Table 2. The differentially expressed (DE)[a] genes identified during pairwise comparisons between the IS compatible and incompatible interactions.

Prot. ID[b]	Putative product or domain [c]	E-Value [d]	Chromosome [e]	IS interactions[f]					
				Com 12h	Com 48h	Com 96h	Incom 12h	Incom 48h	Incom 96h
12 hours post contact									
313750	ferric reductase transmembrane component 5 (*S. hirsutum,* EIM88523)	0	03:2393337-2395631	43.47	50.64	96.53	16.12	24.09	91.85
181229	glycoside hydrolase family 61 protein A (*H. parviporum*, AFO72232)	1.60E-105	10:1078454-1079647	192.06	187.73	521.51	71.75	102.07	106.83
127284	family s53 protease (*S. hirsutum*, EIM82265)	0	04:620130-622362	101.03	156.5	76.73	39.96	53.89	58.49
456720	alpha beta-hydrolase (*G. trabeum*, EJU01112)	0	01: 1226696-1229130	143.96	242.3	596.67	63.44	122.37	162.21
81064	laccase 16 (*S. hirsutum*, EIM86036)	0	10:1682568-1685382	56.86	32.96	56.96	104.69	64.63	130.69
446121	terpenoid synthase (*A. gallica,* AGR34199)	0	09:1234708-1236067	41.18	28.35	29.19	78.51	40.82	44.19
314041	hypothetical protein (S. lacrymans,EGO01877)	0	03:1083564-1086122	52.73	30.00	39.42	101.9	62.22	53.34
163798	cytochrome p450 (*C. subvermispora*, EMD35209)	2.92E-180	09:385741-387743	22.91	8.54	24.28	44.75	18.52	31.72
442228	alcohol oxidase (*S. hirsutum*, EIM82222)	6.55E-126	12:329163-332048	150.42	45.09	69.87	299.78	95.77	134.64
411342	NAD-P-binding protein (*S. hirsutum*, EIM88722)	2.42E-152	09:1554536-1555838	127.44	95.82	164.32	256.37	150.37	166.17
324885	nad-p-binding protein (*C. subvermispora*, EMD40352)	6.93E-90	09:1248476-1249942	88.34	33.69	44.88	184.78	63.57	46.85
45002	carotenoid ester lipase precursor (*S. hirsutum*, EIM86239)	0	05:2480158-2482633	461.39	159.72	529.23	982.37	266.45	692.25
454193	terpenoid synthase (*A. gallica*, EIM91236)	0	09:1246392-1247746	226.62	62.42	71.35	493.98	153.45	158.06
442873	hypothetical protein (*S. commune*, XP003026432)	1.88E-29	01: 625960-626486	412.27	426.4	510.53	916.08	672.24	114.07
151291	alcohol oxidase (*S. hirsutum,* EIM82222)	4.57E-88	07:1116342-1119327	24.09	8.28	12.34	55.00	19.59	26.35
431496	hypothetical protein (*G. trabeum,* EPQ54493)	0	01: 1503902-1506053	23.72	9.64	23.37	54.48	19.27	25.19
67496	cytochrome p450 (*C. subvermispora,* EMD35209)	0	09:1221790-1223847	291.63	92.92	201.02	673.84	222.79	328.17
319809	ctg1 protein (*S. hirsutum,* EIM90876)	3.20E-18	06:665304-665792	21.02	17.17	27.08	50.75	36.16	17.73
479381	hypothetical protein (*C. cinerea,* XP001836190)	9.28E-81	09:1253638-1255194	346.19	86.42	491.13	843.10	242.06	541.55
35202	laccase (*S. hirsutum,* EIM85733)	0	03:2845487-2847947	19.66	10.72	9.94	48.02	19.53	14.86
108168	nad-binding protein (*S. lacrymans,* EGN94562)	8.00E-83	13:326254-327597	139.7	40.53	42.58	343.19	103.45	97.32
455442	predicted protein (*L. bicolor,* XP001881724)	1.86E-08	12:334962-335627	521.06	130.7	371.78	1298.32	385.49	594.46

51706	terpenoid synthase (*A. gallica,* EIM91236)	2.61E-144	05:300390-301759	58.98	15.97	15.15	158.63	48.77	31.47
243529	predicted protein (*L. bicolor,* XP001878385)	1.72E-16	02:296598-297171	15.73	5.51	3.83	43.83	11.16	7.04
106207	hmg-i hmg-y dna-binding conserved site protein (*F. radiculosa,* CCM06252)	8.10E-35	11:1416171-1416699	30.86	31.86	19.20	90.14	105.26	4.25
430720	hypothetical protein (*S. hirsutum,* EIM79696)	1.12E-05	13:507814-508664	148.17	75.69	170.02	465.76	257.77	205.46
48 hours post contact									
127284	family s53 protease (*S. hirsutum,* EIM82265)	0	04:620130-622362	101.03	156.50	76.73	39.96	53.89	58.49
442094	NAD-P-binding protein (*S. hirsutum,* EIM87945)	4.32E-95	11:1063604-1065070	57.35	175.69	190.2	38.21	66.29	113.67
472015	cytochrome P450 monooxygenase 2 (*S. hirsutum,* EIM88596)	0	03:505260-507571	219.14	562.09	797.33	167.02	224.5	343.56
156301	hypothetical protein (*C. subvermispora,* EMD40107)	6.74E-138	05:1060070-1061124	168.51	186.51	411.13	118.43	80.84	476.78
148210	cytochrome p450 (*F. radiculosa,* CCM02682)	1.78E-156	12:80417-82739	50.45	61.86	9.12	24.47	27.32	14.67
108448	no hit	no hit	14:659548-660747	41.52	46.61	15.28	25.59	22.12	29.50
478777	glutathione s-transferase (*S. lacrymans,* EGN97111)	1.46E-109	08:2160242-2161157	120.25	94.61	158.76	134.37	175.20	199.37
442228	alcohol oxidase (*S. hirsutum,* EIM82222)	6.55E-126	12:329163-332048	150.42	45.09	69.87	299.78	95.77	134.64
155921	linoleate diol synthase (*S. hirsutum,* EIM86629)	0	08:650189-655077	234.75	70.29	151.78	352.02	166.61	229.13
454193	terpenoid synthase (*A. gallica,* EIM91236)	0	09:1246392-1247746	226.62	62.42	71.35	493.98	153.45	158.06
428719	hypothetical protein (*P. strigosozonata,* EIN12441)	1.41E-47	08:1300683-1301199	59.22	25.34	352.56	75.61	63.15	257.20
326179	hypothetical protein (*S. hirsutum,* EIM79660)	2.18E-05	09:120939-121800	341.58	105.36	607.25	597.41	276.56	873.69
482307	predicted protein (*L. bicolor,* XP001884826)	4.61E-53	13:1255368-1256154	304.00	93.01	257.70	619.39	259.87	695.72
455442	predicted protein (*L. bicolor,* XP001881724)	1.86E-08	12:334962-335627	521.06	130.7	371.78	1298.32	385.49	594.46
454740	thaumatin-like protein (*S. commune,* XP003030993)	3.61E-24	10:1336937-1337436	14.41	6.80	27.61	32.34	42.24	66.48
96 hours post contact									
452516	no hit	no hit	06:2211772-2212473	37.42	54.98	77.21	49.15	38.33	14.52
108660	plasma-membrane proton-e (*S. lacrymans,* EGN91849)	0	14:14636-19662	18.58	23.25	66.52	20.80	22.08	13.94
315818	other 1 protein kinase (*G. trabeum,* EPQ53938)	2.01E-13	04:765491-765956	8.60	11.51	20.31	7.44	5.71	4.31
106207	hmg-i hmg-y dna-binding conserved site protein (*F. radiculosa,* CCM06252)	8.10E-35	11:1416171-1416699	30.86	31.86	19.2	90.14	105.26	4.25

442873	hypothetical protein (*S. commune,* XP003026432)	1.88E-29	01: 625960-626486	412.27	426.4	510.53	916.08	672.24	114.07
319489	hypothetical protein (*C. subvermispora,* EMD37740)	0	06:365993-367518	7.01	6.71	43.37	5.54	6.33	10.11
149771	glycoside hydrolase family 18 protein (*D. squalens,* EJF66447)	0	01: 2826540-2829119	21.58	25.01	157.68	16.57	19.22	45.51
330334	hypothetical protein (*G. trabeum,* EPQ53120)	8.33E-22	12:705221-705935	63.32	76.20	113.64	97.30	90.34	39.14
412343	phosphatases ii (*S. hirsutum,* EIM87605)	5.90E-61	12:1672429-1673177	99.73	153.24	214.5	111.1	115.44	79.61
445244	hypothetical protein (*T. versicolor,* EIW62825)	6.97E-76	06:1221750-1222854	48.77	55.59	142.56	102.92	68.73	54.17
35909	glutamate decarboxylase (*S. hirsutum,* EIM86926)	0	08:800739-802904	526.9	453.27	912.07	550.8	505.13	348.2
412581	Aldo/keto reductase (*S. hirsutum,* EIM83990)	3.65E-89	13:1128647-1129025	47.67	48.5	105.44	57.02	56.06	40.91
457678	hypothetical protein (*S. hirsutum,* EIM89672)	6.59E-155	02:2996719-2998143	38.77	38.39	154.46	66.1	64.29	60.06
67689	aryl-alcohol oxidase-like protein (*F. mediterranea,* EJD00209)	0	13:872487-875269	20.56	32.75	31.57	9.02	13.66	12.32
67199	glycoside hydrolase family 47 protein (*S. hirsutum,* EIM88924)	0	09:371704-374209	10.33	9.88	61.01	11.05	9.36	24.43
245547	no hit	no hit	07:1215362-1216820	47.84	62.5	104.78	41.51	43.69	43.22
441964	hypothetical protein (*S. hirsutum,* EIM84939)	1.34E-126	11:283126-285081	200.82	196.46	977.64	235.16	289.05	412.74
315263	carbohydrate esterase family 16 protein (*S. lacrymans,* EGN93505)	2.10E-62	04:991582-992161	38.23	41.38	130.22	36.69	34.62	56.35
243347	hypothetical protein (*S. lacrymans,* EGO02924)	4.21E-49	08:186034-186771	55.34	51.84	78.35	56.29	39.96	37.84
240731	staphylococcal nuclease domain-containing protein 1 (*S. hirsutum,* EIM81136)	4.43E-129	06:1996279-1997689	59.81	73.77	270.93	70.77	63.66	132.05
435860	no hit	no hit	09:655123-656608	398.73	289.68	574.61	609.21	381.11	282.85
418625	hypothetical protein (*F. mediterranea,* EJD02639)	4.17E-52	06:1073148-1074676	421.29	416.71	417.98	420.9	405.06	210.70
308718	c2-domain-containing protein (*S. hirsutum,* EIM82273)	3.66E-25	02:274253-274595	72.78	75.83	40.52	96.83	78.68	77.54
318153	60s ribosomal protein l23 (*P. placenta,* XP002471959)	4.42E-78	05:1061912-1063408	83.48	77.08	35.50	92.77	79.86	68.06
419909	no hit	no hit	08:421524-423692	142.71	132.43	101.02	145.47	172.6	194.8
460782	immunomodulatory protein (*F. mediterranea,* EJD00474)	1.84E-17	11:399645-400730	38.44	52.68	52.46	31.97	45.89	101.35
379299	FAD/NAD (P,)-binding domain-containing protein (*S. hirsutum,* EIM91768)	0	02:995276-997840	55.36	38.95	62.81	56.26	49.82	121.89
307924	alpha beta-hydrolase (*C. subvermispora,* EMD32541)	3.68E-98	01:22345-23602	49.78	70.11	24.80	41.23	48.25	48.20
419604	no hit	no hit	07:1633092-1633353	143.96	106.4	95.87	207.87	233.55	210.61
169836	cytochrome c peroxidase (*S. hirsutum,* EIM81294)	0	06:2228660-2230403	196.40	197.83	77.67	177.98	194.36	175.82
108168	nad-binding protein (*S. lacrymans,* EGN94562)	8.00E-83	13:326254-327597	139.70	40.53	42.58	343.19	103.45	97.32
33224	hydrophobin 2 (*H. annosum,* ABA46362)	5.83E-40	06:277914-278512	437.73	336.89	1063.21	702.4	416.53	2477.68

453765	hypothetical protein (*P. carnosa,* EKM52506)	2.63E-08	08:2094771-2095585	95.55	56.88	23.79	137.06	57.73	56.87
453887	cytochrome c oxidase assembly protein (*F. pinicola,* EPT04847)	6.21E-94	09:217087-218504	24.58	19.68	30.72	26.18	31.30	81.42
481675	hypothetical protein (*S. hirsutum,* EIM87659)	0	12:1482430-1484219	157.87	118.70	62.74	120.96	123.63	195.71
326305	alcohol oxidase (*S. hirsutum,* EIM82222)	0	09:1224614-1227167	31.66	15.19	9.07	53.66	25.28	32.52
453889	Peptidase S9A (*F. pinicola*, EGX45765)	1.04E-15	09:221135-224502	110.24	78.26	152.68	160.26	250.29	622.57
174466	glycoside hydrolase family 28 protein (*F. mediterranea,* EJD03462)	1.34E-169	11:306877-308482	1.42	0.85	2.04	5.41	9.86	13.67
328280	plant expansin (*S. hirsutum,* EIM82407)	3.53E-39	11:139101-139832	8.86	7.73	8.09	34.67	59.50	76.90
327286	phosphoglycerate mutase-like protein (*S. hirsutum,* EIM86685)	0	10:1264341-1266133	12.27	13.28	5.49	28.43	21.52	54.21

[a] Genes were considered DE if they displayed a two-fold change in expression at a Benjamini-Hochberg false discovery rate (FDR) cutoff value of 0.05 (i.e., FDR $q \leq 0.05$; and at a 2.0 fold change) (Benjamini and Hochberg, 1995.)

[b] JGI protein identity number.

[c] BLAST2GO (http://www.blast2go.org) was used to annotate the DE genes in each cluster.

[d] BLAST Expect values obtained with BLAST2GO. "No hit" indicated that no homologous sequences were detected in any of the databases searched.

[e] Genome location of the DE genes in the annotated *H. irregulare* reference genome (Olson et al., 2012; DOE Joint Genome Institute, JGI, http://genome.jgi.doe.gov/). The first two digits represent the chromosome on which the gene is located and the numbers following it indicates the nucleotide position on the chromosome.

[f] Expression values are indicated in RPKM (Reads Per Kilobase per Million mapped reads).

Figure 2. Differentially expressed (DE) genes involved in intersterility (IS) in Heterobasidion. Within each circle, are indicated the number of expressed and DE (underlined boldface) genes based on the comparisons between IS compatible and IS incompatible interactions per time point (A). Venn diagram of the comparison of differentially expressed (DE) genes among the time points for each set of interactions based on RNAseq data; in other words, genes that are expressed differentially between each set of time points are included in the shared areas (B). DE genes were identified using Baggerley's Z test (Baggerly et al., 2003) and displayed a two-fold change in expression at a Benjamini-Hochberg false discovery rate (FDR) cutoff value of 0.05 (i.e., FDR q ≤ 0.05; and at a 2.0 fold change) (Benjamini and Hochberg, 1995.) In each case the DE genes represented a subset of the transcripts that were considered expressed (i.e, those detected

above a threshold of 1 count per million [RPKM values ≥ 0.1] with at least 3 mapped unique gene reads) (Wickramasinghe et al., 2012).

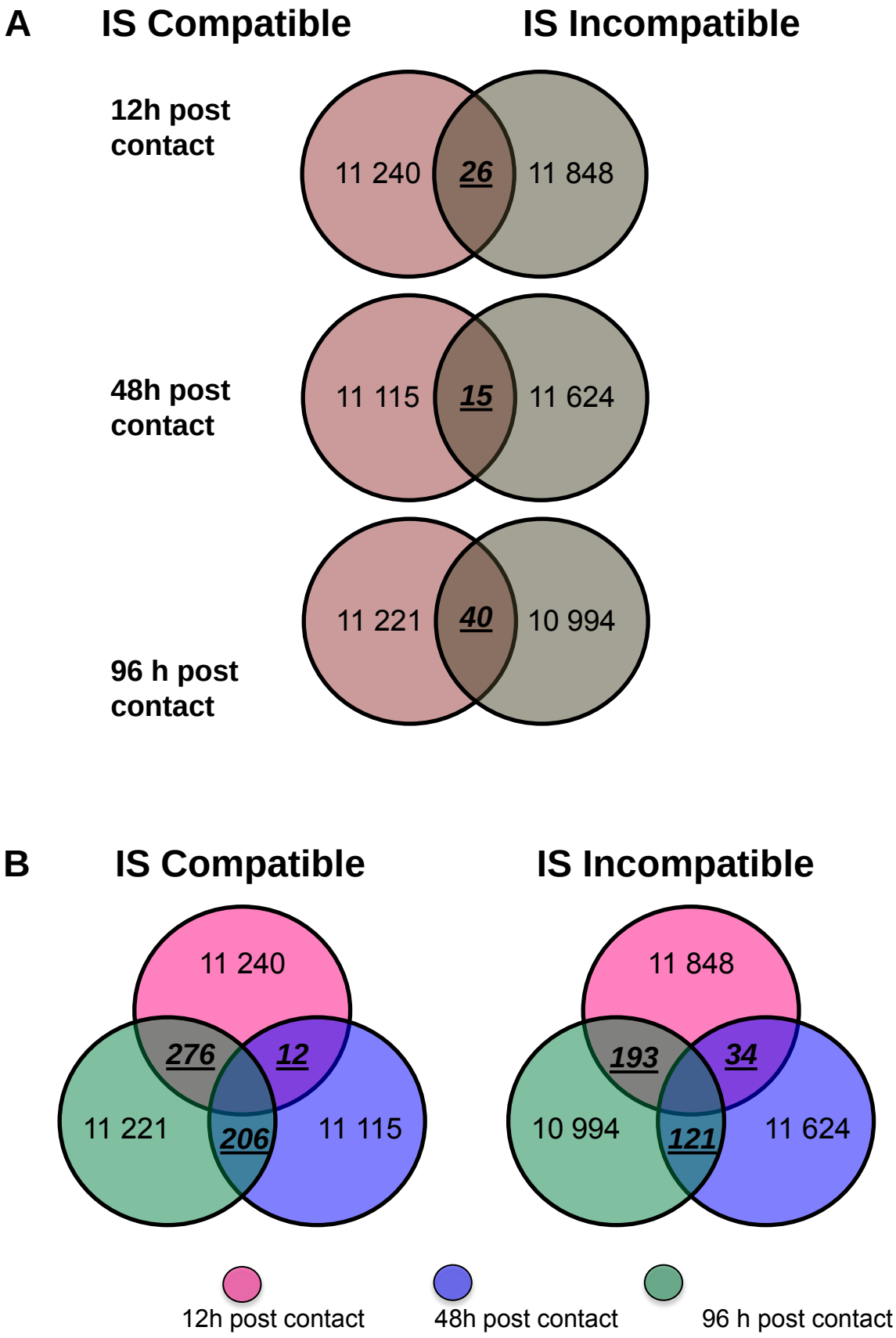

Approximately 85 % of the genes known in *Heterobasidion* were expressed during the course of this study (Supplementary Table 1). A transcript was considered expressed, if it was detected above a threshold of 1 count per million (RPKM values ≥ 0.1) and at least 3 unique gene reads mapped to it (Wickramasinghe et al., 2012). Of the expressed genes, only 724 were DE, as they displayed a 2.0 fold change at an FDR of $q \leq 0.05$ during pairwise comparisons across the various time points and between the IS compatible and incompatible interactions (Supplementary Table 2). For the IS compatible interactions we identified a total of 494 DE genes across the various time points and a total of 348 DE genes across the various time points for the IS incompatible interactions (Supplementary Table 2; Fig. 2). Pairwise comparisons of the IS compatible and incompatible interactions identified 26 DE genes at 12 h after hyphal contact that were not shared between the interaction types, 15 DE genes at 48 h after hyphal contact and 40 DE genes at 96 h after hyphal contact (Fig. 2, Table 2). Among others, these genes encoded putative glycoside hydrolases, terpenoid synthases, alcohol oxidase, cytochrome p450 monooxygenases, laccases, proteases and a cytochrome c peroxidase (Table 2).

Of the DE genes, 34 were highly expressed (i.e., had RPKM values of more than 1000) (Burke et al., 2012) (Supplementary Table 3). Some of these genes were highly expressed early in both the IS compatible and incompatible responses (e.g., genes that encoded a putative cytochrome 5 and class I glutamine amidotransferase-like protein), while others were highly expressed late in both the IS compatible and incompatible responses (e.g., two genes that encoded putative hydrophobins, a gene that encoded a putative glycoside hydrolase family protein 61 and a gene that encoded a putative endoglucanase). Some of the genes were highly expressed early in the IS incompatible responses (e.g., the genes that encoded a putative 1 concacamycin induced protein c and an expansin-like protein), while other genes were highly expressed late in the IS incompatible response (e.g., a gene that encoded a putative aegerolysin and a putative glycoside hydrolyse family 5 protein). We also identified genes that were highly expressed early in the IS compatible response (e.g., a gene encoding a putative aldehyde dehydrogenase), as well as genes that were highly expressed late in the IS compatible response (e.g., a putative heat shock protein 9).

3.2. Gene clustering and Functional annotation

Gene Cluster separated the 724 DE genes into two main clusters (Clusters 1 and 2) each with 3 sub-clusters (A-C) (Fig. 3, Supplementary Table 2). The largest gene cluster, Cluster 1A (230 genes), contained genes that showed high levels of expression during the early time points

Figure 3. A dendrogram and heat map generated with Gene Cluster version 3.0 (de Hoon et al., 2004) showing an overview of the relative expression of the differentially expressed (DE) genes during intersterility (IS) in Heterobasidion. The data was median-centred and the results visualized with TreeView version 1.6.6 (Page, 1996). Expression levels at the three time points (12 h, 48 h and 96 h) for the IS compatible and incompatible interactions were depicted as heat maps (red indicates high expression and green represent low expression). GO terms (Biological Process category) of the 724 unique DE genes in the 6 identified clusters are indicated in the panel next to the heat map.

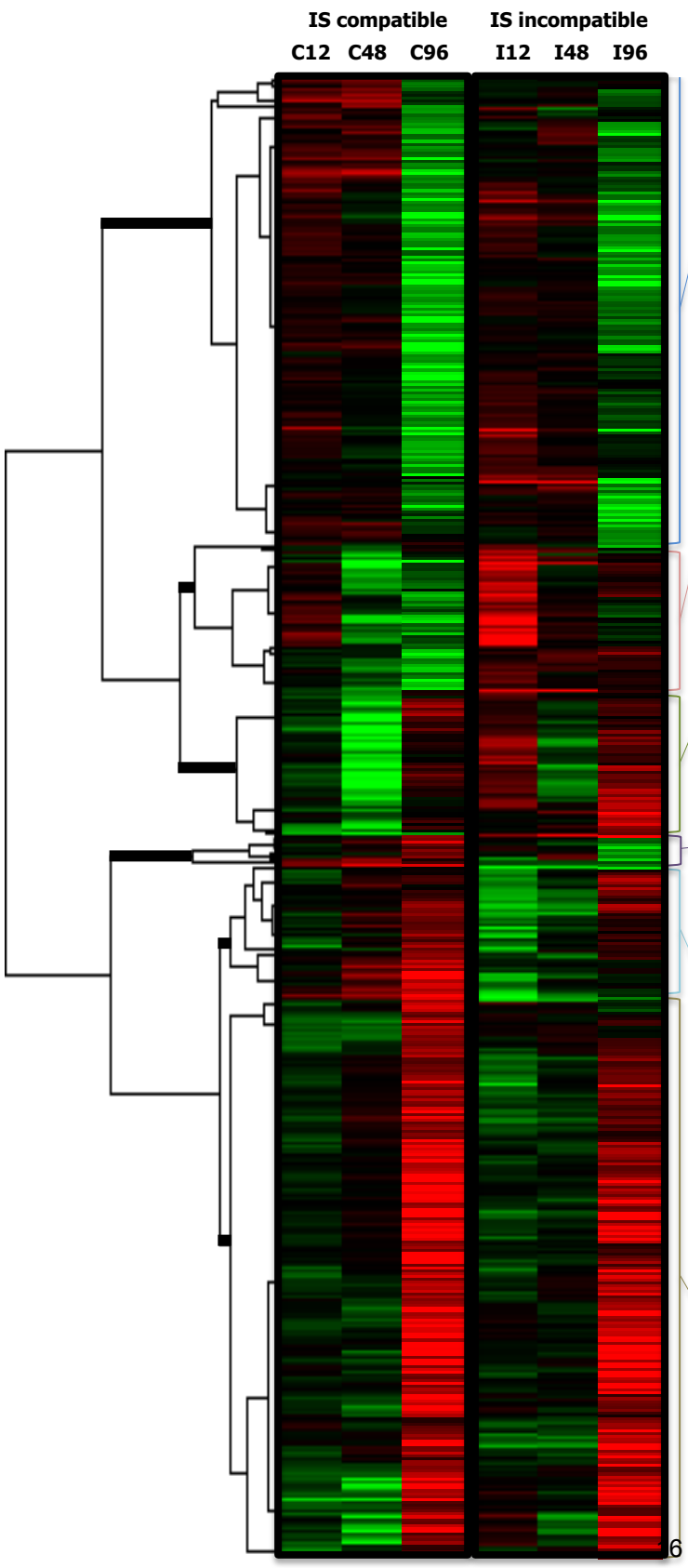

Cluster 1A

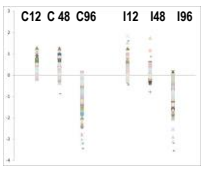

Cellular component biogenesis, Lipid metabolic process, Metabolic process, Arginine catabolic process, Protein N-linked glycosylation via asparagine, Heme metabolic process, Antibiotic biosynthetic process

Cluster 1B

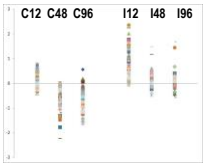

Response to stress , Autophagy, Electron transport, Chitin catabolic process, Alcohol metabolic process , Lipid metabolic process

Cluster 1C

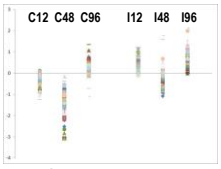

Interspecies interaction between organisms, Reproductive system development, Electron transport, Carbohydrate metabolic process

Cluster 2A

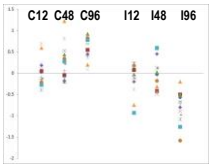

Macromolecule metabolic process, Glutamate metabolic process, Protein dephosphorylation

Cluster 2B

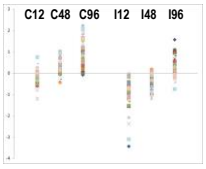

Cellular process, Carbohydrate metabolic process, Nucleic acid transport, DNA catabolic process, Arginine catabolic process

Cluster 2C

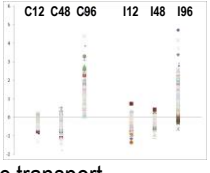

Cell wall biogenesis, Carbohydrate transport, Carbohydrate metabolic process, Regulation of oxidoreductase activity, Electron transport, Organic hydroxy compound metabolism, Tyrosine metabolism, Vacuole organization, Reproduction

(12 and 48 h), while showing decreased levels of expression at 96 h after hyphal contact in both the IS compatible and incompatible interactions (referred to as the early upstream response cluster) (Fig. 3). Cluster 1B (72 genes) and Cluster 1C (69 genes) appeared to harbour genes induced during the IS incompatible response (referred to as the IS incompatible response clusters) (Fig. 3). The genes in Cluster 1B were generally highly expressed in the IS incompatible interactions at 12 h after hyphal contact, while the genes present in Cluster 1C were generally highly expressed at 12 and 96 h after hyphal contact in the IS incompatible interactions in comparison with the IS compatible interactions. Cluster 2A (15 genes) and Cluster 2B (65 genes) included genes induced during mating and sexual development (referred to as the mating and sexual development clusters). The genes present in Cluster 2A were highly expressed at 12, 48 and 96 h after hyphal contact in the compatible interactions, while the genes in Cluster 2B generally showed a late induction in only the compatible interactions in comparison with the IS incompatible interactions. The genes contained in Cluster 2C (273 genes) were most highly expressed 96 h after hyphal contact in both compatible and incompatible IS interactions (referred to as the downstream IS response cluster) (Fig. 3).

The DE genes contained in Cluster 1A (i.e., the genes that showed high levels of expression during the early time points and decreased levels of expression at 96 h after hyphal contact in both the IS compatible and incompatible interactions) were enriched for Biological Process (BP) GO terms associated with "protein-DNA complex subunit organization", DNA conformation change", "lipid metabolic process" and "cellular component organization or biogenesis" (Fig. 3, Supplementary Table 4). Consistent with biological processes associated with biogenesis and metabolism, the cellular components of these GO terms were "macromolecular complex" and "cytoplasmic part" (Supplementary Table 6). Several genes in this cluster also encoded proteins associated with DNA organization (e.g., nucleotide excision repair TFIIH, subunit TTDA, Histone H3 and Histone H4), as well as lipid metabolism (e.g., lipase, NUDIX hydrolase, isopentenyldiphosphate isomerase, cyclopropane-fatty-acyl-phospholipid synthase and a SGNH hydrolase) (Supplementary Table 7). Cluster 1A was enriched with several Molecular Function (MF) GO terms associated with "NADH dehydrogenase (quinone) activity", "oxidoreductase activity", "isopentenyl-diphosphate delta-isomerase activity", "nitrate reductase (NADH) activity", "aldehyde dehydrogenase [$NAD(P)^+$] activity", as well as "nucleotide binding" (Supplementary Table 5).

The DE genes contained in the IS incompatibility response clusters (Clusters 1B and 1C)

were enriched for BP GO terms involved in "cellular response to extracellular stimulus" and "response to stress", especially "response to oxidative stress" (Supplementary Table 4). Genes in these clusters also encoded proteins that may function as chaperones (e.g., a putative HSP20-like and cyclophilins) and that are associated with the stress response (e.g., protein rds1p, glutathione s-transferase, cytochrome c oxidase assembly protein, mismatched base pair and cruciform DNA recognition protein, aldo keto reductase, FAD/NAD(P)-binding domain-containing protein, L-ascorbate oxidase and copper radical oxidase) (Supplementary Table 7). Clusters 1B and 1C were also enriched for BP GO terms that are associated with "autophagy" and "vacuole organization", "oxidation reduction process", "alcohol metabolic process", "isoprenoid metabolic process", "developmental process involved in reproduction" and "lipid biosynthetic process". Consistent with an IS incompatibility response, BLAST2GO and REVIGO identified enriched BP GO terms that are associated with "cell killing", "modification of morphology or physiology of other organism", "disruption of cell of other organism", "interactions with host" (Fig. 4). Cluster 1C was also enriched for BP GO terms that are associated with "reproductive system development", as this cluster included a proteins that are linked with reproduction and fruit body senescence (Sakamoto et al., 2006). Both clusters were enriched for MF GO terms associated with "laccase activity", "catalytic activity" and "electron transport", as well as Cellular Component (CC) GO terms associated with "cell wall" and "external encapsulating structure" (Supplementary Table 6). Consistent with these findings, several DE genes encoded putative proteins that form part of the electron transfer process.

The DE genes contained in the mating and sexual development clusters (Clusters 2A and 2B) were enriched for BP GO terms associated with "protein metabolic process", "DNA catabolic process", "RNA localization", "mRNA transport" and "carbohydrate metabolism", as well as MF GO terms associated with "peptidase activity", "glutamate metabolism", "hydrolyse activity" and "alpha-mannosidase activity" (Supplementary Table 4). Consistent with proteins associated with metabolic and carbohydrate processes, numerous genes in these clusters encoded proteases (e.g., a putative peptidase s28, acid protease, family s53 protease, subtilisin-like proteases and proline-specific peptidase) (Supplementary Table 8) and carbohydrate active enzymes (e.g. glycosyltransferases, endocellulases and endoglucanases) (Supplementary Table 9). For Cluster 2B, the CC GO enrichment terms also pointed to cellular components associated with "extracellular region" and "myosin complex" (Supplementary Table 7).

The DE genes contained in the downstream IS response cluster Cluster 2C were enriched for BP GO terms associated with "cell wall organization", "carbohydrate transport", "carbohydrate

Figure 4. Functional classification summary for Cluster 1C (Biological Process category) represented as a scatter plot using the GO visualization tool REViGO. X- and Y-axes represent a two-dimensional annotation space derived from a multi-dimensional scaling procedure used on a matrix of GO terms' semantic similarities (see reference 51 for details). By employing this visualization method, similar functional categories will cluster together. Bubble colour indicated the user-provided P-values obtained from the GO term enrichment analysis and bubble size relates to the frequency of GO terms in the Gene Ontology Annotation Database.

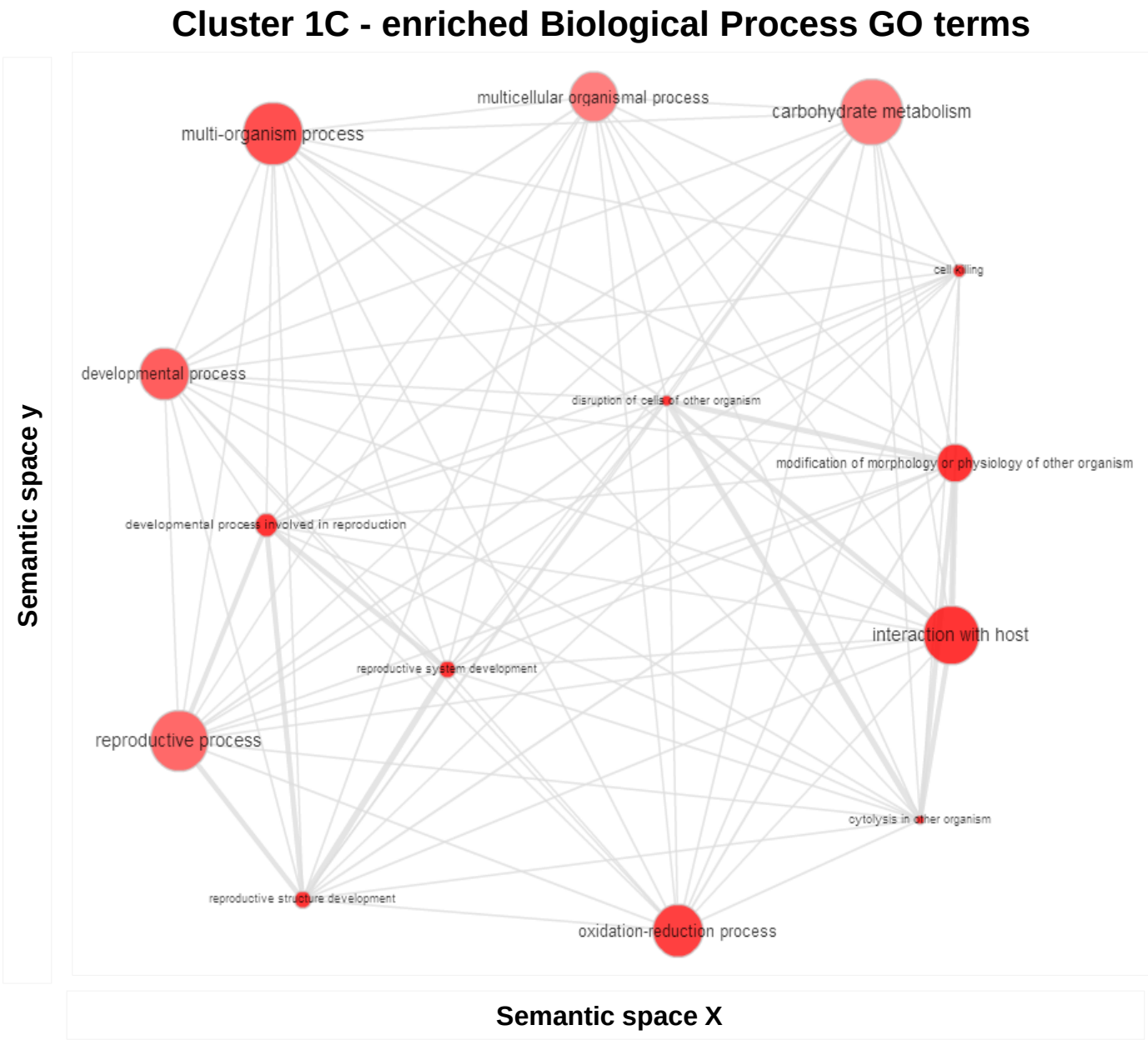

metabolic process", "regulation of oxidoreductase activity", "electron transport", "organic hydroxy compound metabolism" and "tyrosine metabolism" (Supplementary Table 4). Consistent with cell wall biogenesis, various genes in this cluster were also predicted to represent carbohydrate active enzymes (Supplementary Table 9) that share homology with proteins in the carbohydrate esterase and polysaccharide lyase families, as well as glycosyltransferases and glycoside hydrolases. The genes were also enriched for BP GO terms associated with "multicellular organismal reproductive processes", as well enriched for MF GO terms associated with "pheromone activity" (Supplementary Tables 4 and 5). Genes in this cluster are also predicted to encode proteins known to be involved in mating (e.g., pheromones), as well as proteins previously associated with mating (e.g., von willebrand factor, aquaporin, lectin and hydrophobin) (Table 3). The genes in Cluster 2C encode putative proteins enriched for cellular components associated with the "cell wall", "external encapsulating structure", "intracellular", "cytoplasm", "protein complex", "macromolecular complex" and "ribonucleoprotein complex" (Supplementary Table 6).

Ten of the DE genes in Cluster 1B, which shared the same expression profile, were tightly clustered in the same region of the *H. irregulare* genome on Chromosome 9 (09:1215576-1257798) (Fig. 5). These 10 genes were highly expressed at 12 h post hyphal contact, with reduced expression levels at 48 and 96 h post hyphal contact in IS compatible and incompatible interactions. They were more highly expressed in IS incompatible interaction in comparison with IS compatible interactions. The genes located in this cluster may be involved in terpene biosynthesis, as they encode putative proteins that function in terpene synthesis (Fig. 5). The online tool antiSMASH 2.0 (antibiotics and Secondary Metabolite Analysis SHell) (Blin et al., 2013) identified 24 putative secondary metabolite biosynthesis gene clusters, one of which was the cluster on Chromosome 9 (Supplementary Table 10, Fig. 5).

Overall, 88 putative *Heterobasidion* homologs that may belong to the cytochrome P450 superfamily of monooxygenases were identified in our study. Phylogenetic analyses separated the *Heterobasidion* CYP sequences into 6 clans (Fig. 6). Only 25 of the 88 *Heterobasidion* CYP homologs were DE during IS (Supplementary Table 11) and were spread across 3 of the 6 identified clans (Fig. 6). Here, 3 of the 8 CYP53 homologs were DE, 3 of the 20 CYP534 homologs were DE, as well as 19 of the 47 CYP64 homologs were DE during IS in *Heterobasidion*. The latter was also the largest clan, containing more than half of the *Heterobasidion* CYP homologs (47 of the 88 *H. irregulare* CYPs).

Figure 5. A candidate terpene biosynthesis cluster associated with cytochrome P450 monooxygenase (CYP) that is involved in intersterility (IS) in Heterobasidion. The cluster was identified using the online tool antiSMASH 2.0 (antibiotics and Secondary Metabolite Analysis SHell) (Blin et al., 2013). The two genes in this region that were not significantly differentially expressed (i.e., polyprenyl synthetase, Prot ID: 126754 and CYP Prot ID: 164132) are not indicated. The top panel graphically represents the respective changes in expression over time in the IS compatible (indicated in blue) and incompatible (indicated in red) interactions (y-axis = Expression value in Reads Per Kilobase per Million mapped reads or RPKM; x-axis = time when mycelium was harvested with the three time points reflecting, respectively, 12, 48, and 96 h post hyphal contact).

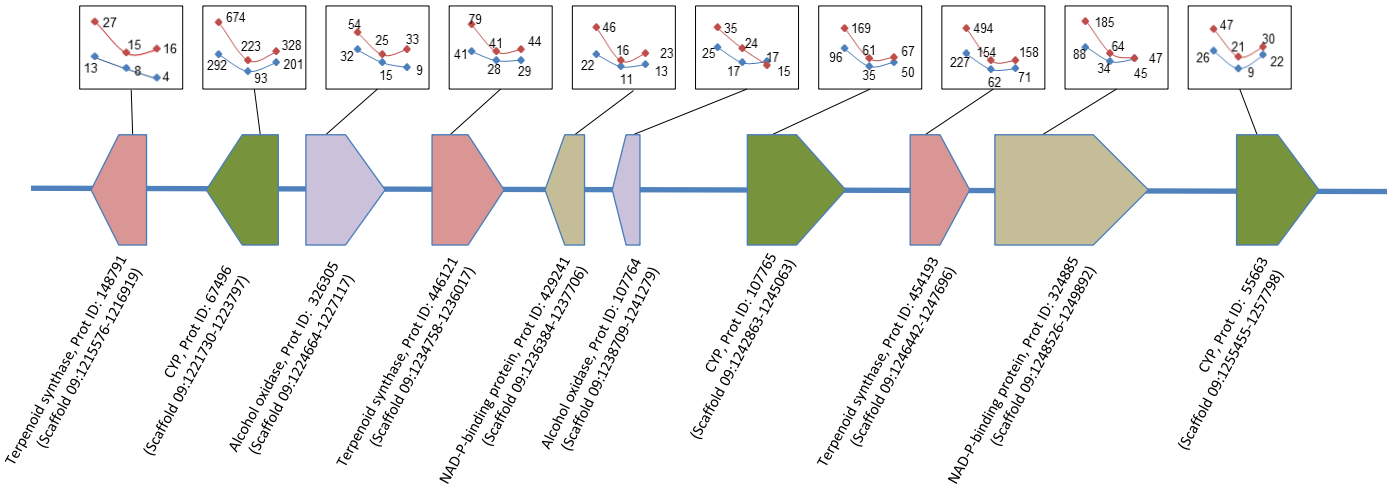

Figure 6. Cytochrome P450 monooxygenase (CYP) dendrogram generated using UPGMA (Unweighted Pair Group Method with Arithmetic mean). The dendrogram was constructed using H. irregulare CYP sequences (indicated as Hetan_Prot IDs) obtained from the JGI database (http://genome.jgi.doe.gov/), as well as previously characterized CYP sequences. These included Phanerochaete chrysosporium (pc, gx and ug), Coprinopsis cinerea (Ccin), Postia placenta (Pp), Neurospora crassa (Ncra), Fusarium oxysprorum (Fox) and Aspergillus nidulans (Asp) (http://drnelson.uthsc.edu/CytochromeP450.html). The sequences were aligned using MAFFT version 7 and the tree constructed using MEGA version 6 (http://www.megasoftware.net) by employing pairwise distances calculated using the Jones-Taylor-Thornton model with gamma correction.

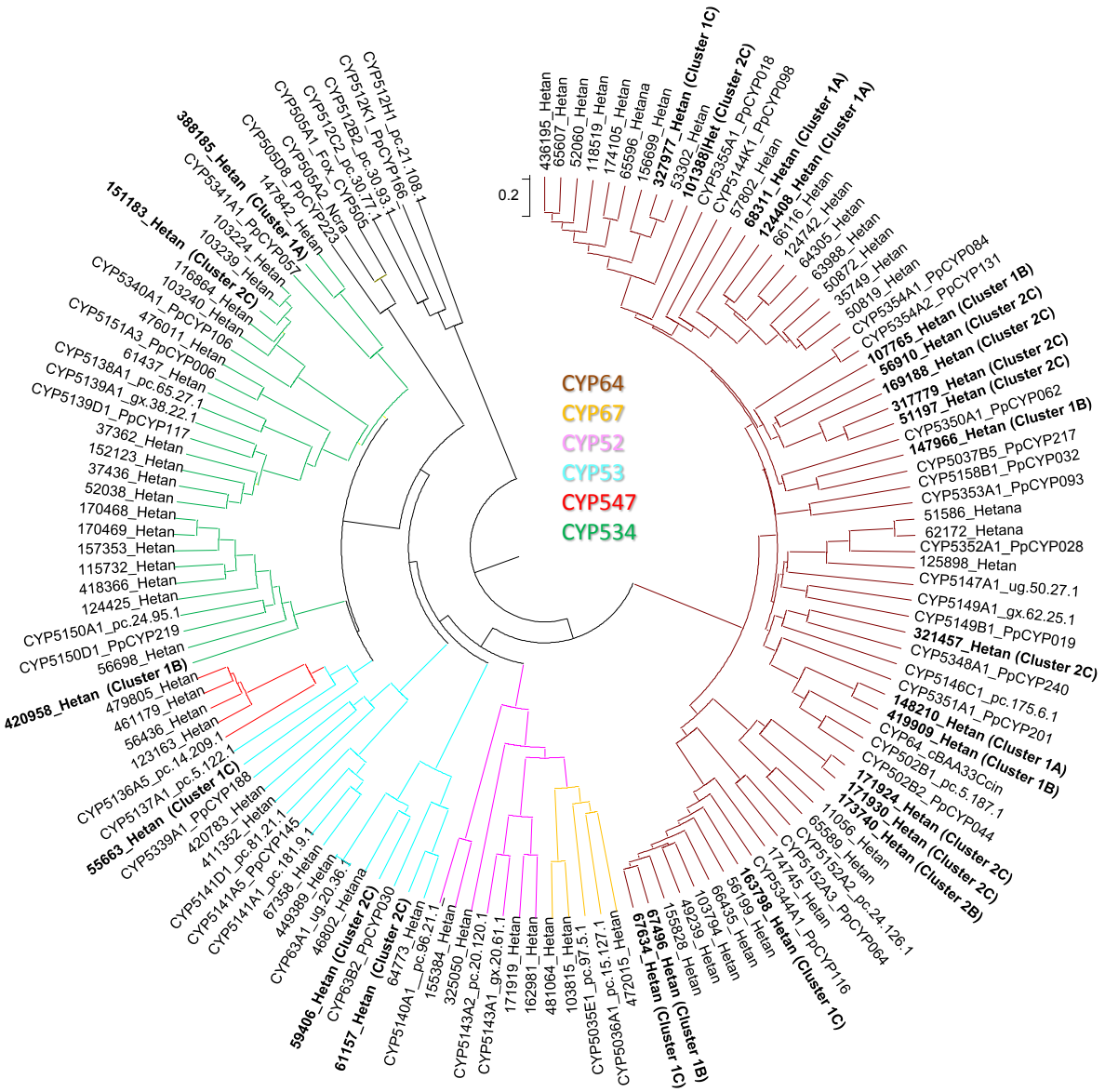

Table 3. Differentially expressed[a] genes encoding putative proteins previously associated with reproductive processes (GO:0032504).

Prot. ID[b]	Cluster[c]	Putative product or domain[d]	E-Value[e]	References	Chromosome[f]	IS interactions[g]					
						Com 12h	Com 48h	Com 96h	Incom 12h	Incom 48h	Incom 96h
181126	2C	Protein with pheromone activity, GO:005186)	no hit	Casselton, Heredity (2002) 88:142–147	07:849217-849448	125.51	161.96	285.3	91.97	140.4	248.23
181275	2C	Protein with pheromone activity, GO:005186)	no hit	Casselton, Heredity (2002) 88:142–147	07:958757-958976	94.54	118.14	191.9	88.9	118.5	215.91
237963	2C	hmg1 protein (S. hirsutum, EIM85725)	1.09E-144	Casselton, Heredity (2002) 88:142–147	03:1405832-1407078	85.62	111.76	200	108.28	110.5	145.02
460226	2C	hmg-protein (*F. pinicola*, EIW54712)	9.19E-45	Casselton, Heredity (2002) 88:142–147	09:190411-192229	92.52	118.87	211.1	67.88	113.5	182.71
438733	2C	c6 transcription factor (*C. subvermispora*, EMD40262)	1.85E-176	G3 (2013) 21:1015-1030	03:39068-41867	61.92	66.14	137.5	65.66	80.29	136.66
415132	2C	c6 transcription (R. solani, CCO27576)	2.98E-12	G3 (2013) 21:1015-1030	02:2902354-2904013	11.95	9.95	39.67	16.17	12.58	31.15
316848	2C	von willebrand domain-containing protein(*S. hirsutum*, EIM90572)	0	Côte et al., MBio 2 (2011): e00230-10.	04:926698-929840	10.1	11.3	27.49	12.01	13.13	27.29
247090	2C	von willebrand factor *(P. indica*, CCA66546)	6.19E-24	Côte et al., MBio 2 (2011): e00230-10.	05:406388-407103	30.25	31.64	170.3	25.08	31.62	142.44
51894	2C	aquaporin (*F. pinicola*, EKM51662)	9.84E-154	Carbrey et al., PNAS (2001) 98:1000–1005	05:968216-969844	33.29	25.25	115.8	35.61	28.43	123.12
58543	2C	cgl3 lectin (*L. amethystine,* BAJ72707)	0	Lakkireddy et al., ICMBMP7 (2011) 82-94	01: 439408-439999	94.25	47.3	947.5	104.44	76.94	1040
455911	2B	reductase akor2 (*S. hirsutum*, EIM83757)	5.52E-151	Coelho et al., PLoS Genet. (2010) 6:e1001052	13:408258-409807	8.96	12.37	24.8	7.09	9.63	10.59
148469	1C	aegerolysin aa-pri1 (*P. ostreatus,* AAL57035)	3.07E-69	Lakkireddy et al., ICMBMP7 (2011) 82-94	04:1415497-1416069	1275.3	268.35	1836	1869.8	723.5	3267.6
38497	1C	erylysin (*P. eryngii,* BAI45248)	0	Lakkireddy et al., ICMBMP7 (2011) 82-94	04:1411975-1414021	220.1	82.93	279.1	336.35	163.4	532.1
156203	1C	fruit-body specific gene c (*S. lacrymans,* EGN98565)	4.69E-80	Sakamoto et al., Plant Physiol. (2006) 141:793–801	05:440823-441637	129.07	64.77	181.2	184.02	97.89	272.7
426840	1C	fruit-body specific gene c (*S. lacrymans,* EGN98565)	1.02E-68	Sakamoto et al., Plant Physiol. (2006) 141:793–801	05:439416-440272	17.19	8.56	22.42	26.08	16.1	43.58
454740	1C	thaumatin-like protein (*S. commune,* XP003030993)	3.61E-24	Sakamoto et al., Plant Physiol. (2006) 141:793–801	10:1336937-1337436	14.41	6.8	27.61	32.34	42.24	66.48
412343	2A	phosphatases ii (*S. hirsutum,* EIM87605)	5.90E-61	Sallee et al., J. Biol. Chem. (2006) 281: 16189-16192	12:1672429-1673177	99.73	153.24	214.5	111.1	115.4	79.61

[a] Genes were considered DE if they displayed a two-fold change in expression at a Benjamini-Hochberg false discovery rate (FDR) cutoff value of 0.05 (i.e., FDR $q \leq 0.05$; and at a 2.0 fold change) (Benjamini and Hochberg, 1995.)

[b] JGI protein identity number.

[c] The differentially expressed genes were clustered based on their expression profile using Gene Cluster version 3.0 identified 6 cluster (Hoon et al., 2004) and named according to Fig. 3.

[d] BLAST2GO (http://www.blast2go.org) was used to annotate the DE genes in each cluster.

[e] BLAST Expect values obtained with BLAST2GO. "No hit" indicated that no homologous sequences were detected in any of the databases searched.

[f] Genome location of the DE genes in the annotated *H. irregulare* reference genome (Olson et al., 2012; DOE Joint Genome Institute, JGI, http://genome.jgi.doe.gov/). The first two digits represent the chromosome on which the gene is located and the numbers following it indicates the nucleotide position on the chromosome.

[g] Expression value (indicated in Reads Per Kilobase per Million mapped reads, or RPKM).

4. DISCUSSION

4.1. RNA-seq reveals the involvement of diverse processes in IS

An RNAseq approach was used for the identification and characterization of gene expression changes associated with IS in *Heterobasidion*. Clustering of the transcripts into six expression profile groups, followed by the application of Gene Ontology (GO) enrichment pathway analysis of each of the clusters allowed inference of biological processes participating in IS. The processes linked with mating compatibility and heterokaryon formation included cell-cell adhesion and recognition, cell cycle control and signal transduction. We also identified processes potentially associated with the restriction of mating and heterokaryon formation between individuals belonging to different species, as well as the activation of programmed cell death (PCD).

4.2. Cell-cell adhesion and plasmogamy represent important steps during IS

Results of this study suggested that cell-cell adhesion, hyphal fusion and heterokaryon formation play central parts in IS in *Heterobasidion*, which is consistent with the idea that IS may regulate anastomosis and plasmogamy (Chase and Ullrich, 1990a). Several DE genes encoded enzymes involved in cell wall degradation and modification, which may play a role in cell-cell adhesion and hyphal fusion (Eyre et al., 2010). These included proteases, as well as carbohydrate-active enzymes (CAZymes) that catalyse formation of glycosidic linkages (e.g., glycosyltransferases) and enzymes mediating their breakdown (e.g., glycoside hydrolases) (e.g., Cantarel et al., 2009). However, cell wall degradation and modification may also be part of the IS incompatible response, as these processes are central to the cell's response during heterospecific non-self recognition (Arfi et al., 2013). For example, the killer toxin-like chitinase *gh18-8* gene in *Neurospora crassa* is induced during self-interactions, as well as during various interspecific interactions (Tzelepis et al., 2012). The gh18-8 protein which is potentially localised in the cell wall is suggested to be part of a nonspecific sensing mechanism in hyphal interactions (Tzelepis et al., 2012). Furthermore, degradation or modification of the cell walls of the opposing individual not only allows entry of toxic or antifungal compounds, but the release of the opponent's cell wall components that can be utilized for nutrition (Hiscox et al., 2010).

Cell-cell adhesion and recognition during IS appears to be influenced by structural factors presented on the cell wall and the extracellular matrix (ECM) of *Heterobasidion*. This is

evident from CC GO enrichment terms associated with the cell wall, extracellular region and external encapsulating structures. Also, several gene products encoded by DE genes are probably located on the cell wall and ECM that influence cell-cell adhesion. These included various aquaporins that influence cell surface properties for substrate adhesion, as well as putative hydrophobins that influence cell-cell adhesion by affecting the ability of hyphae to adhere to hydrophobic surfaces (Zhang et al., 2011; Ahmadpour et al., 2014). In addition, hydrophobins may also be involved in protection against lytic enzymes (Adomas et al., 2006). The cell wall- and ECM-associated proteins that were identified in this study to be involved in the IS response in *Heterobasidion* are consistent with what has been found for interactions between *Phlebiopsis gigantea* and *H. parviporum* (Adomas et al., 2006).

Our data further highlight the importance of cell cycle control for ensuring that interacting partners are in a synchronous stage in order to allow for plasmogamy and heterokaryon formation (Heimel et al., 2010; Erdmann et al., 2012). Several DE genes encoded proteins involved in cell cycle control, which include a putative high mobility group (HMG) I/Y conserved site protein (Reeves, 2000), a putative protein phosphatase 2C (PP2C) family member (Begum et al., 2011), as well as a putative glucosylceramide that are known to regulate the cell cycle and G2/M (gap 2/mitotic) transition (Mouton and Venable, 2000). We also identified a DE gene with homology to the *Rbf1* of *Ustilago maydis*, which has been shown to encode the master regulator of the *mat-B* dependent transcriptional cascade required for *mat-B* induced G2 cell cycle arrest (Heimel et al., 2010). As expected, these putative cell cycle control genes were significantly expressed in both IS compatible and incompatible interactions, since both types of interaction utilize the same initial steps.

4.3. The IS response involves a balance between toxin production and detoxification

The *Heterobasidion* IS interactions investigated here were associated with changes in reactive oxygen species (ROS) and redox status, which is typical for fungal-fungal interactions (Iakovlev and Stenlid, 2000; Iakovlev et al., 2004; Hiscox et al., 2010; Arfi et al., 2013). Not only were several of the GO terms associated with oxidoreductase activity and electron transport, numerous of the DE genes (e.g., quinone oxidoreductases, glutathione S-transferases and CYPs) encode products with homology to proteins that change or influence the redox status (Olson et al., 2012; Arfi et al., 2013). Several DE genes also encoded proteins that form part of the mitochondrial electron transport chain, including proteins that form part of

complexes I and III that have been recognized as major cellular generators of ROS (Dröse and Brandt, 2008). We further identified DE genes that encoded the main oxidative enzymes secreted by *H. irregulare* (e.g., all 6 of the laccases) (Olson et al., 2012), which were previously linked to inter-specific fungal interactions in *Daedalea quercina* and *Trametes versicolor* (Baldrian, 2004; Hiscox et al., 2010).

ROS can react with various cellular components to reduce cell integrity, as well as generate chemically reactive cleavage products (e.g., aldehydes, ketones) (Charizanis et al., 1999; Sunkar et al., 2003). It was therefore not surprising that GO terms associated with 'response to external stimulus' and 'response to stress (especially to oxidative stress)' were enriched during IS in *Heterobasidion*. Numerous DE genes also encoded products homologous to stress response proteins (heatshock protein like 20-like protein, glutathione S-transferases), proteins that have antioxidative activity (peroxiredoxin and taurine dioxygenase), as well as proteins involved in detoxification (haloacid dehalogenase and dihydroxyacetone kinase) (Sunkar et al., 2003; Molin et al., 2003; Chen et. al., 2008; Morsy et al., 2010; Kroll et al., 2013). DE genes encoding laccase and peroxidases could also function to limit ROS damage, by removing H_2O_2 or generating melanins that protect hyphae from ROS and can absorb toxic compounds (Hiscox et al., 2010).

Our findings suggest that IS induced an overall change in the metabolic flux. For example, there were indications of a redirection of the metabolic flux from glycolysis to the pentose phosphate pathway, possibly as part of the oxidative stress response (Grant, 2008; Kroll et al., 2013). Indeed, one of our DE genes encoded a putative phosphoglycerate mutase-like protein (PGAM) that is thought to cause a switch from glycolysis to the pentose phosphate pathway (Shalom-Barak and Knaus, 2002). However, it is also possible that *Heterobasidion* adapts its metabolism to obtain the extra nicotinamide adenine dinucleotide phosphate (NADPH) needed during stress by redirecting carbohydrate fluxes from glycolysis to the pentose phosphate pathway (Grant, 2008). Such a redirection of carbohydrate fluxes is considered as one of the conserved post-translational responses to oxidative stress (Grant, 2008).

Changes in secondary metabolism appear to be fundamental to IS in *Heterobasidion*, which is consistent with previous observations for heterospecific interactions (e.g., Eyre et al., 2010; Hiscox et al., 2010). This is evident in that certain DE genes encoded proteins (e.g., farnesyl-diphosphate synthase) involved in secondary metabolite production (e.g., terpenoids) (Liu et

al., 1999). In addition, we also identified a potential terpene biosynthesis cluster, of which many genes were DE during IS incompatibility. Several of the identified DE genes also encoded putative CYPs, including members of the CYP64 and CYP547 clans known to be involved in the biosynthesis of secondary metabolites (Doddapaneni et al., 2005; Moktali et al., 2012). Previous studies also found that CYPs were DE during heterospecific interactions between *P. gigantea* and *H. parviporum* (Adomas et al., 2006; Hansson et al., 2012[a,b]). Because secondary metabolites potentially confer a competitive advantage to the producer of the compounds (e.g., CYP64 members in *Aspergillus* species produce aflatoxins) (Bhatnagar et al., 2003), certain of the *Heterobasidion* DE CYPs may also be involved in detoxification of secondary metabolites and toxins. For example, members of CYP63 (that was also identified here) was previously shown to be involved in the degradation of xenobiotic compounds during IS (Syed and Yadav, 2012).

4.4. Signal transduction cascades regulate IS

Results of this study thus suggest that several signalling cascades may influence the outcome of IS in *Heterobasidion*. As expected, the genes located at the *mat-A* and *mat-B* loci controlling mating and heterokaryon formation were expressed during the IS compatible and incompatible interactions of *Heterobasidion*. The genes encoding putative pheromones located at the *mat-B* locus showed an increase in expression levels at 72 h after hyphal contact, similar to what was previously observed during mating in *Coprinopsis cinerea* (Erdmann et al., 2012). The putative STE6-C6 transcription factor required for secretion of the mating pheromones also displayed increased expression 72 h after hyphal contact. However, DE of the pheromone receptor genes were not detected, which is probably due to the fact that we only started our transcriptome studies at 24 h post contact and might have missed the peak of their expression that likely occurred much earlier (Erdmann et al., 2012). Results of this study therefore confirmed the role that the *mat* genes, as well as genes required for their secretion, play a role in triggering the signalling cascade needed for mating and heterokaryon formation during IS in *Heterobasidion*.

Our findings suggest that IS in *Heterobasidion* might rely on cAMP-dependent protein kinase A (PKA), as well as mitogen-activated protein kinase (MAPK) signalling, similar to the signalling pathways regulating mating in other fungi (Erdmann et al., 2012). Evidence for the role of cAMP signalling is that one of the DE genes encoded a putative nitrogen metabolite repression protein A (NMRA)/NMRA-like protein 1 (NMRAL1), which modulates the expression of extracellular cAMP and relay genes during cell-cell adhesion in the social

amoeba *Dictyostelium discoideum* (Garciandia and Suarez, 2013). Also, one of the DE genes encoded a putative transcription factor Rst2 that with a decrease in PKA activity, increases the expression of the MAPK kinase kinase (MAPKKK) Ste11, which is essential for induction of sexual development (Sugimoto et al., 1991). It is thus likely that the pheromone response during IS in *Heterobasidion* induces the signalling cascades involving PKA and MAPK, similar to what was observed during mating in *U. maydis* (Heimel et al., 2010).

The compounds produced during IS could trigger signalling cascades that influence the outcome of IS. For example, changes in ROS can function as "redox messengers" in intracellular signalling that regulate the cellular responses to oxidative stress (Circu and Aw, 2010). The putative DE gene homolog of cytochrome c peroxidase, which perceives changes in the concentrations of ROS during IS, could activate transcription factors that are involved in the response to oxidative stress (Charizanis et al., 1999). The breakdown of cell wall components can also be part of a signalling response that in turn activate stress and defence responses during IS. For example, it was demonstrated in plants that pectin degradation/modification could affect cell wall integrity and lead to activation of a stress response (Pelloux et al., 2007), while in *Botrytis cinerea*, cell wall breakdown products serve as a signal for laccase formation and excretion (Marbach et al., 1985). Various signalling pathways may therefore be part of the IS response, similar to what was found to be involved in homospecific non-self recognition (somatic incompatibility) (Hutchison et al., 2009).

Some of the DE genes encoded proteins that might be involved in the activation of programmed cell death (PCD) linked with IS, since the ROS and oxidative stress induced during IS may be downstream effectors of PCD (Hutchison et al., 2009). For example, the DE genes that encoded a putative nicotinamide adenine dinucleotide (NADH):ubiquinone oxidoreductase (known as Mitochondrial Complex 1) could cause mitochondrial DNA damage and activate PCD, as has previously been demonstrated in yeast (Stefanatos and Sanz, 2011). Mitochondrial Complex 1 also controls the relative levels of NAD^+ and NADH that cause glyco- and lipoxidative-damage that can trigger PCD (Stefanatos and Sanz, 2011). We also detected evidence for ketone production during IS through the identification of putative a hydroxymethylglutaryl-coenzyme A synthase and hydroxymethylglutaryl-coenzyme A lyase, which are fundamental components of ketogenesis (Yi et al., 2010). Although ketones can lead to the production of ROS and cause increased lipid peroxidation and growth inhibition, they can also induce mitochondrial permeabilization that increases oxidative stress and induce PCD

(Zago et al., 2000). Additionally, we identified homologs of genes (e.g., ceramide synthase) previously associated with the activation of PCD during homospecific non-self recognition (van der Nest et al., 2011), as well as proteins known to be involved in fruit body senescence (e.g., aegerolysins, a fruit-body specific gene c and thaumatin-like protein) (Sakamoto et al., 2006). Among the *Heterobasidion* DE genes we also identified a putative lectin with homology to the *C. cinerea* galectin *cgl3* that has been shown to regulate cell adhesion and survival (He and Baum, 2006; Wälti et al., 2008). Similar to what has been observed in *Trichoderma* where lectin-carbohydrate interactions triggers the parasitic response (Inbar and Chet, 1995), lectin-carbohydrate interactions might also trigger the reaction cascade associated with the IS incompatibility response and PCD associated with it.

4.5. IS-associated molecular responses are analogous to those elicited during hetero- and homospecific non-self recognition

Based on the overall findings of this study and the data from previous work, we propose a model for the key events that occur during IS in *Heterobasidion* (Fig. 7). Similar to the mating response, cell wall modification and cell cycle control allow for hyphal fusion, plasmogamy and heterokaryon formation during IS in *Heterobasidion*. These events are most likely regulated by the pheromone response and MAPK cascades needed for mating and heterokaryon formation (Erdmann et al., 2012). Although certain events are shared during the mating and IS responses in *Heterobasidion*, our data confirmed that IS incompatibility overrides the mating response (Chase and Ullrich, 1990a; Iakovlev et al., 2004). This is consistent with the inference that incompatible IS interactions were associated with an increase in ROS levels and the production of secondary metabolites and extracellular enzymes, as well as the activation of stress responses. Our data thus suggest that processes similar to those previously associated with heterospecific non-self recognition (e.g., mycoparastism) (e.g, Iakovlev and Stenlid, 2000; Iakovlev et al., 2004; Adomas et al., 2006; Baldrian 2004; Hiscox et al., 2010) and homospecific non-self recognition (e.g., somatic incompatibility) (van der Nest et al., 2011; Paoletti and Saupe, 2009; Bidard et al., 2013), underlie IS incompatibility in *Heterobasdion*. We therefore posit that IS in *Heterobasidion* represents a type of non-self recognition system that protects the individual from other organisms, including closely related species.

Figure 7. Model for the molecular processes underpinning intersterility (IS) in Heterobasidion. Based on the overall findings of this study and the data from previous work, we propose a model of key events that occur during IS compatible and incompatible interactions in Heterobasidion. ECM = Extracellular Matrix; ROS = Reactive Oxygen Species; PCD = Programmed Cell Death.

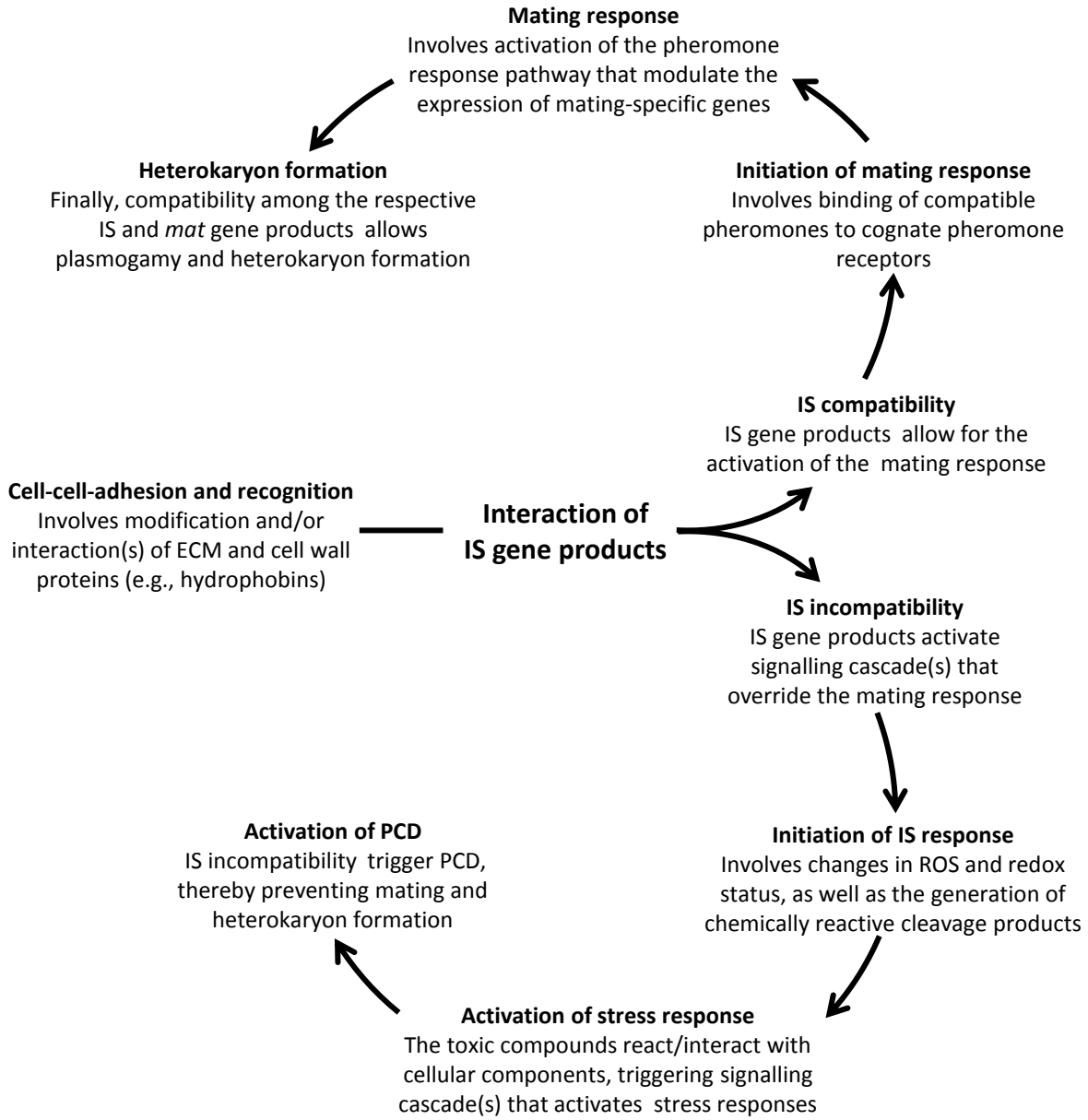

4.6. Future prospects

This study represents the first genome wide investigation on the molecular basis of IS in fungi. Although transcriptional studies have traditionally been reserved for genetic model organisms (Vijay et al., 2013), the use of RNAseq allowed genome wide analysis of transcriptional changes induced during IS in the non-model fungus *Heterobasidion*. The identification and functional annotation of DE genes facilitated significant improvements in our knowledge regarding transcriptional responses to intersterility in *Heterobasidion*, and in general, to self/non-self recognition processes in fungi.

The findings presented here are valuable for future investigations into the molecular mechanisms underlying IS in this and other fungi. Two future avenues for research would be to mine the RNAseq data to characterize the IS loci in *Heterobasidion* and to improve genome annotations for members of this taxon. In terms of genome annotations, RNAseq data are exceptionally useful for defining 5′ and 3′ untranslated regions of mRNAs, exon/intron boundaries, and splice variants, etc. (Liu et al., 2012). Characterization of the IS loci could potentially be accomplished using the combined information generated in this study and those from previous studies where these loci were positioned on genome-anchored genetic linkage maps (Olson et al., 2012; Lind et al., 2012). The RNAseq data can then be used to assess allele-specific expression and to identify eQTLs (expression quantitative trait loci) (Pirinen et al 2014). Information regarding transcript abundance of genes surrounding these loci during IS interactions may also help identify IS genes or genes involved in IS. The exact role of these genes in IS and the general biology of *Heterobasidion* can then be explored using gene disruption experiments (Samils et al., 2006). Incorporation of these data using a systems biology approach involving genomics, transcriptomics, proteomics, metabolomics and epigenomics will ultimately provide a comprehensive understanding of the molecular mechanisms underlying IS in *Heterobasidion* and its broader role in the biology of this fungus.

5. ACKNOWLEDGEMENTS

We thank the National Research Foundation, the Swedish Foundation for Strategic Research and the Swedish Research Council for Environment, Agricultural Sciences and Spatial Planning (Uppsala Microbiomics Center) for financial support

REFERENCES

1. Adomas, A., Eklund, M., Johansson, M., Asiegbu, F.O., 2006. Identification and analysis of differentially expressed cDNAs during nonself-competitive interaction between *Phlebiopsis gigantea* and *Heterobasidion parviporum*. FEMS Microbiol. Ecol. 57, 26–39.
2. Ahmadpour, D., Geijer, C., Tamas, M.J., Lindkvist-Petersson, K., Hohmann, S., 2013. Yeast reveals unexpected roles and regulatory features of aquaporins and aquaglyceroporins. Biochim. Biophys. Acta. 1840, 1482-1491.
3. Arfi, Y., Levasseur, A., Record, E., 2013. Differential gene expression in *Pycnoporus coccineus* during interspecific mycelial interactions with different competitors. Appl. Environ. Microbiol. 79, 6626-6636.
4. Baggerly, K., Deng, L., Morris, J., Aldaz, C., 2003. Differential expression in SAGE: Accounting for normal between-library variation. Bioinformatics. 19, 1477-1483.
5. Baldrian, P., 2004. Purification and characterization of laccase from the white-rot fungus *Daedalea quercina* and decolorization of synthetic dyes by the enzyme. Appl. Microbiol. Biotechnol. 63, 560–563.
6. Begum, N., Shen, W., Manganiello, V., 2011. Role of PDE3A in regulation of cell cycle progression in mouse vascular smooth muscle cells and oocytes: Implications in cardiovascular diseases and infertility. Curr. Opin. Pharmacol. 11, 725-729.
7. Bendz-Hellgren, M., Stenlid, J., 1997. Decreased volume growth of *Picea abies* in response to *Heterobasidion annosum* infection. Can. J. Forest Res. 27, 1519–1524.
8. Benjamini, Y., Hochberg, Y., 1995. Controlling the false discovery rate: A practical and powerful approach to multiple testing. J. Roy. Stat. Soc. B. 57, 289–300.
9. Bhatnagar, D., Ehrlich, K.C., Cleveland, T.E., 2003. Molecular genetic analysis and regulation of aflatoxin biosynthesis. Appl. Microbiol. Biotechnol. 61, 83-93.
10. Bidard, F., Clavè, C., Saupe, S.J., 2013. The transcriptional response to non-self in the fungus *Podospora anserina*. G3. 3, 1015-1030.
11. Blin, K., Medema, M.H., Kazempour, D., Fischbach, M.A., Breitling, R., Takano, E., Weber, T., 2013. AntiSMASH 2.0 - A versatile platform for genome mining of secondary metabolite producers. Nucleic Acids Res. 41(W1), W204-W212.
12. Burke, G.R., Strand, M.R., 2012. Deep sequencing identifies viral and wasp genes with potential roles in replication of *Microplitis demolitor* bracovirus. J. Virol. 86, 3293-3306.
13. Cantarel, B.L., Coutinho, P.M., Rancurel C., Bernard, T., Lombard, V., Henrissat, B., 2009. The Carbohydrate-Active EnZymes database (CAZy): An expert resource for glycogenomics. Nucleic Acids Res. 37, D233-D238.

14. Charizanis, C., Juhnke, H., Krems, B., Entian, K.D., 1999. The mitochondrial cytochrome c peroxidase Ccp1 of *Saccharomyces cerevisiae* is involved in conveying an oxidative stress signal to the transcription factor Pos9 (Skn7). Mol. Gen. Genet. 262, 437-447.
15. Chase, T.E., 1986. Genetics of sexuality and speciation in the fungal forest pathogen *Heterobasidion annosum*. University of Vermont. Dissertation 1986.
16. Chase, T.E., Ullrich, R.C., 1990[a]. Five genes determining intersterility in *Heterobasidion annosum*. Mycologia. 82, 73–81.
17. Chase, T.E.. Ullrich. R.C., 1990[b]. Genetic basis of biological species in *Heterobasidion annosum*: Mendelian determinants. Mycologia. 82, 67-72.
18. Chen, L.R., Markhart, A.H., Shanmugasundaram, S., Lin, T.Y., 2008. Early developmental and stress responsive ESTs from mungbean, *Vigna radiata* (L.) Wilczek, seedlings. Plant Cell Rep. 27, 535-552.
19. Circu, M.L., Aw, T.Y., 2010. Reactive oxygen species, cellular redox systems, and apoptosis. Free Radical Bio. Med. 48, 749-762.
20. Conesa, A., Götz, S., García-Gómez, J.M., Terol, J., Talón, M., Robles, M., 2005. Blast2GO: A universal tool for annotation, visualization and analysis in functional genomics research. Bioinformatics. 21, 3674-3676.
21. de Hoon, M.J.L., Imoto, S., Nolan, J., Miyano, S., 2004. Open Source Clustering Software. Bioinformatics. 20, 1453-1454.
22. Degner, J.F., Marioni, J.C., Pai, A.A., Pickrell, J.K., Nkadori, E., Gilad, Y., Pritchard, J.K., 2009. Effect of read-mapping biases on detecting allele-specific expression from RNA-sequencing data. Bioinformatics. 25, 3207-3212.
23. Doddapaneni, H., Chakraborty, R., Yadav, J.S., 2005. Genome-wide structural and evolutionary analysis of the P450 monooxygenase genes (P450ome) in the white rot fungus *Phanerochaete chrysosporium*: Evidence for gene duplications and extensive gene clustering. BMC Genomics. 6, 92.
24. Dröse, S., Brandt, U., 2008. The mechanism of mitochondrial superoxide production by the cytochrome bc1 complex. J. Biol. Chem. 283, 21649-21654.
25. Erdmann, S., Freihorst, D., Raudaskoski, M., Schmidt-Heck, W., Jung, E-M., Senftleben, D., Kothe, E., 2012. Transcriptome and functional analysis of mating in the basidiomycete *Schizophyllum commune*. Eukaryot. Cell. 11, 571-589.
26. Eyre, C., Muftah, W, Hiscox, J., Hunt, J., Kille, P., Boddy, L., Rogers, H.J., 2010. Microarray analysis of differential gene expression elicited in *Trametes versicolor* during interspecific mycelial interactions. Fungal Biol. 114, 646-660.

27. Garbelotto, M., Gonthier, P., Linzer, R., Nicolotti, G., Otrosina, W., 2004. A shift in nuclear state as the result of natural interspecific hybridization between two North American taxa of the basidiomycete complex *Heterobasidion*. Fungal Genet. Biol. 41, 1046–1051.
28. Garbelotto, M., Gonthier, P., Nicolotti, G., 2007. Ecological constraints limit the fitness of fungal hybrids in the *Heterobasidion annosum* species complex. Appl. Environ. Microb. 73, 6106-6111.
29. Garciandia, A., Suarez T., 2013. The NMRA/NMRAL1 homologue PadA modulates the expression of extracellular cAMP relay genes during aggregation in *Dictyostelium discoideum.* Dev. Biol. 381, 411–422.
30. Grant, C.M., 2008. Metabolic reconfiguration is a regulated response to oxidative stress. J. Biol. 7, 1.
31. Hansen, K.D., Irizarry, R.A, Zhijin, W.U., 2012. Removing technical variability in RNA-seq data using conditional quantile normalization. Biostatistics. 13, 204-216.
32. Hansson, D., Menkis, A., Himmelstrand, K., Thelander, M., Olson, Å., Stenlid, J., Karlsson, M., Broberg, A., 2012[a]. Sesquiterpenes from the conifer root rot pathogen. *Heterobasidion occidentale*. Phytochemistry. 82, 158-165.
33. Hansson, D., Menkis, A., Olson, Å., Stenlid, J., Broberg, A., Karlsson, M., 2012[b]. Biosynthesis of fomannoxin in the root rotting pathogen *Heterobasidion occidentale*. Phytochemistry. 84, 31-39.
34. He, J., Baum, L.G., 2006. Galectin interactions with extracellular matrix and effects on cellular function. Methods Enzymol. 417, 247–56.
35. Heimel, K., Mario Scherer, M., Schuler, D., Kämpera, J., 2010. The *Ustilago maydis* Clp1 protein orchestrates pheromone and b-dependent signaling pathways to coordinate the cell cycle and pathogenic development. The Plant Cell. 22, 2908–2922.
36. Heitman, J., Kronstad, J.W., Taylor, J.W., Casselton, L.A., 2007. Sex in Fungi: Molecular determination and evolutionary implications, ASM Press, Washington, DC.
37. Hiscox, J., Baldrian, P., Rogers H.J., Boddy, L., 2010. Changes in oxidative enzyme activity during interspecific mycelial interactions involving the white-rot fungus *Trametes versicolor*. Fungal Genet. Biol. 47, 562–571.
38. Huang, W., Khatib, H., 2010. Comparison of transcriptomic landscapes of bovine embryos using RNA-Seq. BMC genomics. 11, 711.
39. Hutchison, E., Brown, S., Tian, C., Glass, N.L., 2009. Transcriptional profiling and functional analysis of heterokaryon incompatibility in *Neurospora crassa* reveals that

ROS, but not metacaspases, are associated with programmed cell death. Microbiol. Papers. 155, 3957-3970.

40. Iakovlev, A., Olson, A., Elfstrand, M., Stenlid, J., 2004. Differential gene expression during interactions between *Heterobasidion annosum* and *Physisporinus sanguinolentus*. FEMS Microbiol. Lett. 241, 79–85.
41. Iakovlev, A., Stenlid, J., 2000. Spatiotemporal patterns of laccase activity in interacting mycelia of wood-decaying basidiomycete fungi. Microb. Ecol. 39, 236–245.
42. Inbar, J., Chet, I., 1995. The role of recognition in the induction of specific chitinases during mycoparasitism by *Trichoderma harzianurn.* Microbiology. 141, 2823-2829
43. Kendziorski, C., Irizarry, R.A., Chen, K.S., Haag, J.D., Gould, M.N., 2005. On the utility of pooling biological samples in microarray experiments. Proc. Natl. Acad. Sci. USA. 102, 4252–4257.
44. Kircher, M., Heyn, P., Kelso, J., 2011. Addressing challenges in the production and analysis of illumina sequencing data. BMC Genomics. 12, 382.
45. Korhonen, K., 1978. Intersterility groups of *Heterobasidion annosum*. Commun. Inst. For. Fen. 94, 25.
46. Korhonen, K., Capretti, P., Karjalainen, R., Stenlid, J., 1998. Distribution of *Heterobasidion annosum* intersterility groups in Europe, in: Woodward, S., Stenlid, J., Karjalainen, R., Hüttermann, A. (Eds.), *Heterobasidion annosum*, Biology, Ecology, Impact and Control. CAB International, Wallingford, Oxon, UK, pp. 93–104.
47. Korhonen, K., Fedorov, N.I., La Porta, N., Kovbasa, N.P., 1997. *Abies sibirica* in the Ural region is attacked by the S type of *Heterobasidion annosum*. Eur. J. Forest Pathol. 27, 273–281.
48. Kroll, K., Pähtz, V., Kniemeyer, O., 2013. Elucidating the fungal stress response by proteomics. J Proteomics. 97, 151-163.
49. Lind, M., Olson, A., Stenlid, J., 2005. An AFLP-markers based genetic linkage map of *Heterobasidion annosum* locating intersterility genes. Fungal Genet. Biol. 42, 519–527.
50. Liu, C.J., Heinstein, P., Chen, X.Y., 1999. Expression pattern of genes encoding farnesyl diphosphate synthase and sesquiterpene cyclase in cotton suspension-cultured cells treated with fungal elicitors. Mol. Plant Microbe In. 12, 1095-1104.
51. Liu, S., Zhang, Y., Zhou, Z., Waldbieser, G., Sun, F., Lu, J., Zhang, J., Jiang, Y., Zhang, H., Wang, X., Rajendran, K.V., Khoo, L., Kucuktas, H., Peatman, E., Liu, Z., 2012. Efficient assembly and annotation of the transcriptome of catfish by RNA-Seq analysis of a doubled haploid homozygote. BMC Genomics 13, 595.

52. Marbach, I., Harel, E., Mayer, A.M., 1985. Pectin, a second inducer for laccase production by *Botrytis cinerea*. Phytochemistry. 24, 2559-2561.
53. Marioni, J.C., Mason, C.E., Mane, S.M., Stephens, M., Gilad, Y., 2008. RNA-seq: An assessment of technical reproducibility and comparison with gene expression arrays. Genome Res. 18, 1509-1517.
54. Moktali, V., Park, J., Fedorova-Abrams, N.D., Park, B., Choi, J., Lee, Y.H., Kang, S., 2012. Systematic and searchable classification of cytochrome P450 proteins encoded by fungal and oomycete genomes. BMC Genomics. 13, 525.
55. Molin, M., Norbeck, J., Blomberg, A., 2003. Dihydroxyacetone kinases in *Saccharomyces cerevisiae* are involved in detoxification of dihydroxyacetone. J. Biol. Chem. 278, 1415-1423.
56. Morsy, M.R., Oswald, J., He, J., Tang, Y., Roossinck, M.J., 2010. Teasing apart a three-way symbiosis: Transcriptome analyses of *Curvularia protuberata* in response to viral infection and heat stress. Biochem. Bioph. Res. Co. 401, 225–230.
57. Mortazavi, A., Williams, B.A., McCue, K., Schaeffer, L., Wold, B., 2008. Mapping and quantifying mammalian transcriptomes by RNA-Seq. Nat. Meth. 5, 621-628.
58. Mouton, R.E., Venable, M.E., 2000. Ceramide induces expression of the senescence histochemical marker, b-galactosidase, in human fibroblasts. Mech. Ageing Dev. 113, 169–181.
59. Möykkynen, T., von Weissenberg, K., Pappinen, A., 1997. Estimation of dispersal gradients of S- and P-type basidiospores of *Heterobasidion annosum*. Eur. J. For. Path. 17, 291-300.
60. Nagalakshmi, U., Wang, Z., Waern, K., Shou, C., Raha, D., Gerstein, M., Snyder, M., 2008. The transcriptional landscape of the yeast genome defined by RNA sequencing. Science. 320, 1344-1349.
61. Olesnicky, N.S, Brown, A.J, Dowell, S.J, Casselton, L.A., 1999. A constitutively active G-protein-coupled receptor causes mating self-compatibility in the mushroom *Coprinus*. EMBO Journal. 18, 2756-2763.
62. Oliva, J., Gonthier, P., Stenlid, J., 2011. Gene flow and inter-sterility between allopatric and sympatric populations of *Heterobasidion abietinum* and *H. parviporum* in Europe. For. Path. 4, 243–252.
63. Olson, Å, Stenlid, J., 2001. Mitochondrial control of fungal hybrid virulence. Nature. 411, 438.

64. Olson, Å., 2006. Genetic linkage between growth rate and the intersterility genes S and P in the basidiomycete *Heterobasidion annosum s.lat.*. Mycol. Res. 110, 979–984.
65. Olson, A., Aerts, A., Asiegbu, F., Belbahri, L., Bouzid, O., Broberg, A., Canbäck, B., Coutinho, P.M., Cullen, D., Dalman, K., Deflorio, G., van Diepen, L.T.A., Dunand, C., Duplessis, S., Durling, M., Gonthier, P., Grimwood, J., Fossda, C.G., Hansson, D., Henrissat, B., Hietala, A., Himmelstrand, K., Hoffmeister, D., Högberg, N., James, T.Y., Karlsson, M., Kohler, A., Kües, U., Lee, Y.-H., Lin, Y-C., Lind, M., Lindquist, E., Lombard, V., Lucas, S., Lundé, K., Morin, E., Murat, C., Park, J., Raffaello, T., Rouzé, P., Salamov, A., Schmutz, J., Solheim, H., Ståhlberg, J., Vélëz, H., de Vries, R.P., Wiebenga, A., Woodward, S., Yakovlev, I., Garbelotto, M., Martin, F., Grigoriev, I.V., Stenlid, J., 2012. Insight into trade-off between wood decay and parasitism from the genome of a fungal forest pathogen. New Phytol. 194, 1001–1013.
66. Otrosina, W.J., Garbelotto, M., 2010. *Heterobasidion occidentale* sp. nov. and *Heterobasidion irregulare* nom. nov.: A disposition of North American *Heterobasidion* biological species. Fungal Biol. 114, 16–25.
67. Page, R.D.M., 1996. TREEVIEW: An application to display phylogenetic trees on personal computers. Computer Appl. Biosci. 12, 357-358.
68. Paoletti, M., Saupe, S.J., 2009. Fungal incompatibility: Evolutionary origin in pathogen defense? BioEssays. 31, 1201–1210.
69. Pelloux, J., Rustérucci, C., Mellerowicz, E.J., 2007. New insights into pectin methylesterase structure and function. Trends Plant Sci. 12, 267-277.
70. Pirinen, M., Lappalainen, T., Zaitlen, N. A., Dermitzakis, E. T., Donnelly, P., McCarthy, M. I., Rivas, M.A., 2014. Assessing allele specific expression across multiple tissues from RNA-seq read data. bioRxiv, 007211.
71. Reeves, R., 2000. Structure and function of the HMGI(Y) family of architectural transcription. Environ. Health Persp. 108, 803-809.
72. Sakamoto, Y., Watanabe, H., Nagai, M., Nakade, K., Takahashi, M., Sato, T., 2006. *Lentinula edodes* tlg1 encodes a thaumatin-like protein that is involved in lentinan degradation and fruiting body senescence. Plant Physiol. 141, 793–801.
73. Samils, N., Elfstrand, M., Lindner-Czederpiltz, D. L., Fahleson, J., Olson, Å., Dixelius, C., Stenlid, J., 2006. Development of a rapid and simple *Agrobacterium tumefaciens*-mediated transformation system for the fungal pathogen *Heterobasidion annosum*. FEMS Microbiology Letters. 255, 82-88.

74. Schroeder, A., Mueller, O., Stocker, S., Salowsky, R., Leiber, M., Gassmann, M., Lightfoot, S., Menzel, W., Granzow, M., Ragg, T., 2006. The RIN: An RNA integrity number for assigning integrity values to RNA measurements. BMC Mol. Biol. 7, 3.
75. Shalom-Barak, T., Knaus, U.G., 2002. A p21-activated kinase-controlled metabolic switch up-regulates phagocyte NADPH oxidase. J. Biol. Chem. 277, 40659-40665.
76. Stefanatos, R., Sanz, A., 2011. Mitochondrial complex I a central regulator of the aging process. Cell Cycle. 10, 1528-1532.
77. Stenlid, J., 1985. Population structure of *Heterobasidion annosum* as determined by somatic incompatibility, sexual incompatibility and isoenzyme patterns. Can. J. Bot. 63, 2268–2273.
78. Stenlid, J., Karlsson, J.-O., 1991. Partial intersterility in *Heterobasidion annosum*. Mycol. Res. 95, 1153-1159.
79. Sugimoto, A., Iino, Y., Maeda, T., Watanabe, Y., Yamamoto, M., 1991. *Schizosaccharomyces pombe* ste11+ encodes a transcription factor with an HMG motif that is a critical regulator of sexual development. Genes and Development. 5, 1990-1999.
80. Sunkar, R., Bartels, D., Kirch, H.H., 2003. Overexpression of a stress-inducible aldehyde dehydrogenase gene from *Arabidopsis thaliana* in transgenic plants improves stress tolerance. The Plant Journal. 35, 452-464.
81. Syed, K., Yadav, J.S., 2012. P450monooxygenases (P450ome) of the model white rot fungus *Phanerochaete chrysosporium*. Crit. Rev. Microbiol. 38, 339–363.
82. Tzelepis, G.D., Melin, P., Jensen, D.F., Stenlid, J., Karlsson, M., 2012. Functional analysis of glycoside hydrolase family 18 and 20 genes in *Neurospora crassa*. Fungal Genet. Biol. 49, 717–730.
83. van der Nest, M.A., Steenkamp, E., Slippers, B., Mongae, A., van Zyl, K., Wingfield, M.J., Wingfield, B.D., 2011. Gene expression associated with vegetative incompatibility *in Amylostereum areolatum*. Fungal Genet. Biol. 48, 1034–1043.
84. van Diepen, L.T.A., Olson, A., Ihrmark, K., Stenlid, J., James, T.Y., 2013. Extensive trans-specific polymorphism at the mating type locus of the root decay fungus *Heterobasidion*. Mol. Biol. Evol. 10, 2286-301.
85. Wälti, M.A., Walser, P.J., Thore, S., Grünler, A., Bednar, M., Künzler, M., Aebi M., 2008. Structural basis for chitotetraose coordination by CGL3, a novel galectin-related protein from *Coprinopsis cinerea*. J. Mol. Biol. 379, 146-159.
86. Wickramasinghe, S., Rincon, G., Islas-Trejo, A., Medrano, J.F., 2012. Transcriptional profiling of bovine milk using RNA sequencing. BMC Genomics. 13, 45.

87. Yi, W., Fu, P., Fan, Z., Aso, H., Tian, C., Meng, Y., Ying, C., 2010. Mitochondrial HMG-CoA synthase partially contributes to antioxidant protection in the kidney of stroke-prone spontaneously hypertensive rats. Nutrition. 26, 1176-1180.
88. Zago, E.B., Castilho R.F., Vercesi, A.E., 2000. The redox state of endogenous pyridine nucleotides can determine both the degree of mitochondrial oxidative stress and the solute selectivity of the permeability transition pore. FEBS Letters. 478, 29-33.
89. Zhang, S, Xia, Y.X., Kim, B., Keyhan, N.O., 2011. Two hydrophobins are involved in fungal spore coat rodlet layer assembly and each play distinct roles in surface interactions, development and pathogenesis in the entomopathogenic fungus, *Beauveria bassiana*. Mol. Microbiol. 80, 811-826.